1967

Static behavior of continuous composite beams, March 1967

J. H. Daniels

J. W. Fisher

LEHIGH UNIVERSITY INSTITUTE OF RESEARCH

Shear Connector Design for Highway Bridges

STATIC BEHAVIOR OF CONTINUOUS COMPOSITE BEAMS

by
J. Hartley Daniels
John W. Fisher

Fritz Engineering Laboratory Report No. 324.2

STATIC BEHAVIOR OF CONTINUOUS COMPOSITE BEAMS

by

J. Hartley Daniels

and

John W. Fisher

This work has been carried out as part of an investigation sponsored jointly by the New York Department of Public Works, the Department of Commerce - Bureau of Public Roads, Nelson Stud Division of Gregory Industries, Inc., KSM Products Division of Ormark Industries, Inc., Tru-Weld Division of Tru-Fit Screw Products, Inc., and Lehigh University.

March 1967

Fritz Engineering Laboratory
Department of Civil Engineering
Lehigh University
Bethlehem, Pennsylvania.

Fritz Engineering Laboratory Report No. 324.2

TABLE OF CONTENTS

ABSTRACT

A previous report (Ref. 5) discussed the behavior of four two-span continuous composite steel-concrete beams which were tested under fatigue loading. In that investigation, each beam was subjected to a certain number of cycles of zero to maximum load. The maximum load was equal to the service load of the beam.

This report discusses the behavior of the same four continuous composite beams which were subsequently tested statically to ultimate load. These tests were made after each beam had been fatigue tested. The purpose of the ultimate strength tests was two-fold: (1) to determine if sufficient shear capacity remained after fatigue testing to develop the flexural strength of the beam, and (2) to further investigate the feasibility of applying the concepts of plastic analysis and ultimate strength theory to the design of continuous composite beams.

This investigation has shown that shear connectors designed on the basis of the static and fatigue requirements suggested in Ref. 4, will provide sufficient shear connection to develop the ultimate flexural strength of the member even after the design cycle life of the connection in fatigue has been reached. On the basis of this investigation, it has also been shown that simple plastic analysis and ultimate strength theory can be used for the design of continuous composite beams. In addition, this investigation indicates that the tensile strength of the longitudinal reinforcement in the slab can be used in the design.

The static tests of the four continuous composite beams have also illustrated that local flange and web buckling of the wide-flange shape adjacent to the interior support can have an effect on the ultimate strength behavior. However, in these tests, the predicted ultimate load capacity of three of the four beams was exceeded even with severe local buckling. In the fourth beam the test load reached 97% of the predicted load.

The test results reported herein clearly show that further studies of flange and web local buckling in continuous composite beams are required.

1.0 INTRODUCTION

Recently, there has been a growing interest in the design of continuous composite steel-concrete beams for bridges and buildings. The determination of the elastic properties of such beams however, has traditionally been a complex problem. Due to cracking of the concrete slab in the negative moment regions, the moment of inertia of the beam will not be constant along a span length. But the extent of the negative moment region (extent of cracking) and the elastic properties of the continuous beam are inter-dependent. Therefore, to determine the point of contraflexure a tedious trial and error design approach is indicated. Designs for moving loads on bridge girders and the presence of slip (incomplete interaction) between the slab and the steel beam further complicates the problem.

A much simpler design approach for continuous composite beam would be the familar plastic method for steel structures, combined with simple rules for determining the ultimate moment of resistance of a cross-section when the slab is in tension or compression. However, safeguards are required to ensure adequate rotation capacity of the positive (slab in compression) and negative (slab in tension) plastic hinges. This means that secondary failures which tend to limit the plastic hinge moment must be prevented. Similar rules and safeguards are in fact necessary to allow the plastic design of steel structures.

It has been well established that ultimate strength concepts may be used to predict the flexural strength of cross-sections of composite beams where the slab is in compression and adequate shear connection is provided.[1] Flexural strength at negative hinge locations, rotation capacity and the prevention of secondary failures are presently the subject of further investigation.

The current design procedure for continuous composite bridge girders[2] is based on the static properties of connectors,[3] and present designs normally omit shear connectors in the negative moment regions. The studies reported in Ref. 3 noted that in negative moment regions only the slab reinforcement can act compositely with the steel beam. It was also noted that since there was no significant difference in the distribution of strains and moments whether or not connectors were placed in the negative moment regions, no special provisions were needed for the design of continuous composite beams. Hence, the specifications[2] noted only that, "In case reinforcement steel embedded in the concrete is not used in computing the section, shear connectors need not be provided in these portions of the spans".

A recently developed procedure for the design of the shear connectors in composite steel-concrete bridge members considers their performance under working loads and their ability to develop the flexural strength of the members.[4] The new design criteria proposed that connectors be provided throughout the length of continuous beams. This was considered necessary because in the negative moment regions of composite beams with continuous longitudinal reinforcement, tensile forces would exist that must be carried by connectors along the beam length. If connectors are not provided throughout the negative moment regions these forces must be carried by connectors near the inflection points and in the positive moment regions. It was suggested that connectors in the negative moment regions were also required in order to maintain flexural conformance and to prevent the sudden transition from a composite to a non-composite section. In addition, these connectors would tend to minimize the large differentials in slip deformation that might otherwise occur which could lead to fatigue failure of connectors adjacent to the negative moment regions.

Laboratory fatigue tests on four full size two-span continuous composite beams were reported in Ref. 5. These tests indicated that connectors are required in the negative moment regions if the shear connection is designed using the provisions of Ref. 4. These tests also indicated that additional longitudinal reinforcement was desirable in the negative moment regions over that currently recommended by the AASHO Bridge Specification.[2]

To provide additional information on the static strength of continuous composite beams, comparative ultimate strength tests were also conducted on the same four continuous composite beams reported in Ref. 5. These tests were made following the fatigue testing of each continuous beam. Two of the beams were identical except that while both beams had shear connectors designed in accordance with the fatigue requirements of Ref. 4, they were placed throughout the beam length in one of the beams and omitted from the negative moment region of the other beam as is commonly done in many current designs. Both beams had identical longitudinal and transverse reinforcement. The amount was made equal to the quantity of longitudinal distribution reinforcement which would be placed in actual bridge decks of similar proportions (Ref. 5). The other two continuous beams were essentially the same as the first two beams but had continuous shear connection designed in accordance with the static requirements of Ref. 4 and substantially more longitudinal reinforcement in their negative moment regions.

Complete details of the design, construction and fatigue testing of the four continuous composite beams has been reported in Ref. 5. The results of the ultimate strength tests of these beams which followed the fatigue tests are the subject of this report. The purpose of the ultimate strength tests was two-fold: (1) to determine if sufficient shear capacity remained to develop the flexural strength of the beam, and (2) to further investigate the feasibility of applying the concepts of plastic analysis and ultimate strength theory to the design of continuous composite beams.

2.0 REVIEW OF PREVIOUS STUDIES ON CONTINUOUS COMPOSITE BEAMS

Viest, Fountain and Siess[3] discussed the negative moment regions of continuous composite bridge beams in some detail. This discussion was based on the static behavior of two composite model bridges that were reported by Siess and Viest.[6] These models differed in that one had shear connectors throughout the beam while the second had shear connectors in the positive moment regions only. From these studies it was concluded that (1) in the negative moment regions, only the slab reinforcement can act compositely with the steel beams; (2) in bridges with shear connectors throughout the beam, the slab reinforcement was fully effective; with connectors omitted from the negative moment region the slab reinforcement was only partly effective, and (3) the action of both of these continuous composite bridges was about the same since the distribution of strains and thus also of moments in both positive and negative moment regions was nearly the same.

Based on these studies, it was concluded that the use of an elastic analysis in combination with the usual load distribution factors is justified, and no special provisions are needed for the design of continuous composite bridges.[3]

Slutter and Driscoll[7] summarized the behavior of a single continuous composite beam tested statically to its ultimate load.[8] The test was conducted to investigate whether or not it would be feasible to apply the concepts of plastic analysis together with ultimate strength theory to the design of continuous composite beams. In the positive moment region, the concrete contributed to the ultimate moment of the cross-section. In the negative moment region only the steel beam plus the reinforcement was considered. Only 0.2% of longitudinal reinforcement was provided throughout the beam length. It was noted in Ref. 7 that the theoretical plastic collapse load was exceeded in the test even though the member theoretically had inadequate shear connection throughout its length. It was further concluded in Ref. 7 that although the feasibility of the plastic design of continuous composite members cannot be fully evaluated from the test of only one member, it appears that members in which the negative plastic hinge forms first could be designed by plastic analysis. It was also stated that beams in which positive plastic hinges form first have not been tested, but plastic analysis of these members would appear to be feasible because the positive plastic hinges undoubtedly have sufficient rotation capacity to permit the formation of a negative hinge. Ref. 8 suggested that only the steel beam be considered effective over the negative moment regions, and suggested expansion joints in the slab to control cracking.

Iwamoto[9] gave a comparative discussion on the design and construction cost of the first continuous composite bridge in Japan. At that time (1962) eleven (assumed) continuous composite girder bridges had been constructed since 1958. In each bridge the concrete slab in the negative moment region had been pre-compressed either by raising and settlement (preloading) or by prestressing with steel wires, or by a combination of the two methods.

Tachibana, Kondo and Ito[10] discussed the behavior of continuous composite beams prestressed with wire cables.

More recently, Barnard and Johnson[11] presented the results of a study on the plastic behavior of continuous composite beams. Inelastic regions or hinges in composite beams were classified as strain-softening (positive hinges) or strain-hardening (negative hinges). From this study it was concluded that, (1) it should be possible to design by the conventional plastic design methods any continuous composite beam in which the strain-softening hinges are the last to form, (2) slip increases deflections, but does not appear to have any effect on the ultimate strength behavior of the beam, (3) the fully plastic moment of the steel alone, based on the minimum yield stresses of the beam and reinforcement steels, is a safe estimate of the moment of resistance at beam collapse of a cross-section in which the concrete slab is in tension. These conclusions presuppose that secondary failures can be avoided.

The most important secondary failures requiring further study were listed in Ref. 11 as (1) longitudinal splitting of the slab, (2) diagonal tension failure of the slab, and (3) buckling of the steel beam. Three other secondary failures were observed in the tests reported in Ref. 11 but they could easily be prevented by appropriate detailing.

The studies reported in Ref. 11 were followed up by further studies designed to provide more information on secondary failures.[12] In particular, the effects of cracking and transverse bending of the slab on the ultimate strength were examined. In addition, an investigation of the behavior of longitudinal reinforcement over the supports was made. Preliminary analysis of the test results suggested that the simple plastic theory can be used for the design of continuous composite beams, and full use can be made of the tensile strength of the longitudinal reinforcement in the slab.

3.0 DESCRIPTION OF TEST BEAMS

The four continuous composite T- beams which were tested to ultimate load were each 50'-10" long. The beams had two equal spans of 25'-0" between bearings. Symmetrical concentrated loads (distributed across the slab width) were placed 10'-0" from the exterior support in each span. Each of the four beams consisted of a reinforced concrete slab 60-in wide and 6-in thick connected to a 21W62 steel beam by pairs of 3/4-in diameter headed stud shear connectors 4-in high. The transverse spacing of studs in each stud pair was 4-in (symmetrical with the W). The rolled beams were all supplied from the same heat of A36 steel. Further description of these test beams and a discussion of the design criteria, design details, fabrication, construction, and fatigue tests, has been reported in Section 3 of Ref. 5. The four beams were designated CC-1F, CC-2F, CC-3S and CC-4S.

Beams CC-1F and CC-2F were designed primarily to provide comparative information on the fatigue behavior of the shear connection under working loads.[5] The shear connection for both beams was designed in accordance with the fatigue requirements of Ref. 4, except that connectors were omitted from the negative moment region of CC-1F. On this basis, the number of connectors available in each beam somewhat exceeded the number which would be required for an ultimate strength design.[4] Fatigue failures of some studs occurred in both beams, especially in beam CC-1F during the fatigue tests. However, adequate shear connection remained for the static tests.

Longitudinal and transverse reinforcement was provided in each beam in accordance with the AASHO Bridge Specification.[2] Flexural stresses in the steel beam were kept close to the AASHO specified allowable stresses to prevent premature failures of the wide-flange cross-section, especially at the interior support of each beam.

The shear connectors in beams CC-3S and CC-4S were proportioned on the basis of the static strength requirements suggested in Ref. 4. These beams had substantially more negative longitudinal reinforcement than beams CC-1F and CC-2F. Although beams CC-3S and CC-4S were designed primarily to provide experimental data on the ultimate strength behavior of continuous composite beams, they were first tested under fatigue loading.

Failures of a few studs also occurred in beams CC-3S and CC-4S during fatigue testing. However, adequate shear connection was available for the subsequent ultimate strength tests, as there was no indication of impending shear failure during these tests. Since Ref. 4 suggests that a reduction factor of 0.85 be used with the static design requirement, some stud failures can be tolerated.

Because local flange buckling was of major importance during the ultimate strength tests of beams CC-1F and CC-2F, it was decided to make a comparative study of the effects of introducing some stiffeners in the region of a possible local flange buckle in beams

CC-3S and CC-4S. The stiffener detail is shown in Fig. 7 of Ref. 5. Only a bearing stiffener was provided over the interior support of beams CC-1F and CC-2F. Additional stiffeners were purposely omitted from beams CC-1F and CC-2F because of fatigue requirements of the steel beam. In beams CC-3S and CC-4S, four full height stiffener plates were provided. These plates were placed at 15" centers each side of the support. Two small bearing stiffeners were placed at the edges of the bearing plate, in addition to a full height bearing stiffener over the support.

So that comparative results of the tests of all four beams could be made, the cross-sections, span lengths and load positions for all four test beams were kept constant. The only variables were the amount of shear connection along the beam, quantity of longitudinal reinforcement in the negative moment regions, and stiffener details. These variables are discussed in detail in Ref. 5.

4.0 PROPERTIES OF THE TEST BEAMS

A detailed test program was conducted to determine the physical characteristics of the materials used in the four continuous composite beams. Also, the physical dimensions were obtained to help ascertain the section properties of the beams. Further descriptions of the cross section properties and the material properties of the rolled steel beams, reinforcing bars, stud shear connectors and the slab concrete has been reported in Section 4 of Ref. 5.

The four rolled steel beams were made of structural carbon steel meeting the requirements of ASTM A36-63T. The beams were all nominally 57-ft in length and furnished from the same heat. The mill report is given in Table 2 of Ref. 5. Mechanical properties of the structural steel were determined from tests of tensile coupons cut from a 2-ft piece of the beam that had been flame cut from the original 57-ft length.

Mechanical properties of the No. 4, 6 and 7 deformed longitudinal reinforcing bars were determined by direct tension tests of 3-ft lengths of reinforcement.

The properties of the stud shear connectors were determined from tensile tests on full sized studs. The studs were supplied by two manufacturers.

Standard 6-in by 12-in cylinders were made of all concrete used in the casting of the slabs. These cylinders were tested at the age of 28 days and at the beginning of each fatigue and static test. The 28 day cylinders were moist cured; all other cylinders were cured under approximately the same curing conditions as the slabs.

The properties of the rolled steel beams, reinforcing bars, stud shear connectors, slab concrete and the cross-section properties are given in Tables 2 to 6 of Ref. 5.

The computed flexural strength in the positive moment regions was equal to 830 k-ft and 809 k-ft for beams CC-1F and CC-2F respectively and 770 k-ft for both beams CC-3S and CC-4S. The flexural strength of the negative moment region was 508 k-ft for both beams CC-1F and CC-2F, 633 k-ft for CC-3S and 737 k-ft for CC-4S. The flexural strength in the positive moment region was computed using the method described in Ref. 7. In the negative moment regions the flexural strength was based on the fully yielded beam and yielded tensile reinforcement.

5.0 INSTRUMENTATION AND TESTING PROCEDURE

5.1 Instrumentation

The instrumentation for beams CC-1F and CC-2F was essentially the same and was planned primarily for the fatigue testing program. For those tests it was desirable to attach electrical resistance strain gages to the steel beam at the load-points, close to the inflection points, and over the center support so that slab forces at these sections could be accurately computed. Bending moments and curvatures were also computed from these strain gage readings. Since beams CC-3S and CC-4S were designed primarily for the ultimate strength tests, the instrumentation was planned with that in mind. Electrical resistance strain gages were kept out of the region of high strains. Mechanical strain gage points were placed in the flange tips of the steel beams at the load-points and over the center support so that accurate curvature data at these sections could be obtained during the entire test. The center reaction was measured with a large 300 kip capacity compression load cell so that accurate bending moments along the beam could be computed.

Deflection measurements under the load points were initially made with two 0.001-in dial gages with 2-in travel. For increased deflection a 6-in graduated scale was used which measured to 0.01-in.

Slip measurements were taken at various locations along the beams with 0.001-in dial gages. Rotation of the beam over each exterior support were measured with level bars and 0.001-in dial gages.

Further details of the instrumentation used for all four continuous beam tests is reported in Section 5 of Ref. 5.

5.2 Test Procedure

Beams CC-1F and CC-2F were each tested under fatigue loading to 2,000,000 cycles of load application using two Amsler alternating stress machines and two Amsler hydraulic jacks. The ultimate strength test of each beam was started from 4(CC-2F) to 8(CC-1F) days after each fatigue test. The same Amsler hydraulic jacks were used to apply the static load. The static load was measured with an Amsler Pendulum Dynamometer which had a maximum load range of 0 to 200 kips per jack.

Beams CC-3S and CC-4S were each tested under fatigue loading to 500,000 cycles of load application. The ultimate strength test of each beam was started from 36(CC-4S) to 59(CC-3S) days after each fatigue test. The same Amsler equipment was used for the fatigue and static tests of these beams.

The ultimate strength test of each beam required two consecutive days to complete. Total testing time ranged from 8 to 12 hours. Loads were increased in relatively small increments during the first day until some plastic deformations had taken place. Increments of load were applied in approximately one to five minutes. Load was then held constant for 20 to 40 minutes while data was obtained from all instruments. During the second day of test, plastic deformation was continued until the ultimate load had been reached and unloading was evident. Generally, 15 to 20 minutes was required to allow the test load to stabilize before data was taken.

As long as the static test load was below the load corresponding to first yielding of the steel beam, increments of load were applied. When it was evident that the load was stable (usually shortly after application of the load increment) data was recorded from all instrumentation. As plastification began (applied load to yield load ratio of 1.0 to 1.25 approximately) a longer interval was required before the applied load stabilized and deflections ceased. In the plastic range, where the load was relatively constant, increments of deflection were applied. Data was recorded only after a sufficient interval had elapsed to allow the load and deflections to stabilize. Since deformation rather than load was being applied, it was thus possible to obtain data up to and beyond maximum load capacity of the beams.

Detailed measurements of slab cracks in the negative moment regions of beams CC-3S and CC-4S were made following each test. A 40 power microscope was used to measure the width of cracks.

Figure 1 shows the four continuous composite beams following the ultimate strength tests. A schematic view of the test set-up is shown in Fig. 11 of Ref. 5. Further discussion of the support details for each beam and a discussion of the bracing used at the ends of the beams has been reported in Section 5 of Ref. 5.

6.0 TEST RESULTS

6.1 Load - Deflection Behavior of the Continuous Beams

Deflection measurements at the two load points of each beam were obtained during the progress of each ultimate strength test. The load - deflection results are summarized in Table 1 and Figs. 2 to 5. The theoretical first yield shown in Table 1 was based on cross-section properties reported in Ref. 5. The analysis considered the change in the moment of inertia along the beam due to cracking of the concrete slab. The point of inflection was computed by trial and error procedures. The theoretical maximum load shown in the Table was computed using the simple plastic theory. The theoretical elastic-plastic load - deflection curves shown in each of the above Figures was also computed from the simple plastic theory. An idealized elastic-plastic stress-strain curve was assumed.

Certain visual observations were made during the progress of each test. These observations are summarized in Figs. 2 to 5 by the letters (A) to (D) as follows:

(A) Approximate indication of first yielding of the the steel beam. Due to residual stresses in the vicinity of welds at stiffener locations, some yield lines were visible during the initial fatigue tests. These lines were mainly confined to the lower regions of the web of the steel beam under the two load-points and to the upper and lower regions of the web over the center support. First yielding was taken as the first indication of definite yielding in the flanges of the steel beam, as evidenced by cracks in the whitewash which covered the steel surface.

(B) Development of an apparent negative plastic hinge at the center support. This stage was considered to have been reached when yielding had progressed approximately to the theoretical plastic centroid of the section. At this point, there were large cracks in the slab in the negative moment region of each beam, and there was considerable tension flange and web yielding under each load point. Local flange and web buckling, introduced additional yield lines which tended to obscure the yield patterns associated with the negative plastic hinge alone. The theoretical formation of the negative plastic hinge is shown by an "X" on the theoretical curves in Figs. 2 to 5.

(C) Lower flange and web of the steel beam began to buckle noticeably adjacent to the center support. Generally, local buckling was observed to begin on both sides of the support, then progress more rapidly on one side. At the conclusion of the tests, the flange which developed the major local buckle was observed to have twisted some 30 to 45 degrees from its original position. The flange on the other side of the support would be only slightly twisted at this time. Figure 6 shows the typical local flange and web buckling which had developed by the end of testing.

(D) The top surface of the concrete slab has begun to crush adjacent to one of the loading beams. Fig. 7 shows the extent of crushing which had occurred at two load points by the end of the test.

In general, it was observed that the beams exhibited a linear load - deflection behavior until first yielding. First yielding always occurred in the bottom flange of the steel beam over the center support. At the apparent formation of the negative plastic hinge (as defined above), yielding under the load points was extensive. Plastic deformations increased rapidly following the formation of the apparent negative plastic hinge at the center support. In each beam the maximum load was determined by crushing of the concrete at the load points; an exception occurred in beam CC-4S where local buckling also occurred at approximately the maximum load.

Near the first attainment of the ultimate load, tensile cracks were observed on the lower face of the slab over the center support. However, as deformations increased and load either was maintained or reduced, these cracks closed. In beams CC-3S and CC-4S, considerable crushing occurred on the lower face on the slab over the center support near the end of the test, thus indicating incomplete interaction. Fig. 8 shows the crushing on the lower face of the slab of beam CC-4S.

In beams CC-1F and CC-4S cracks also formed on the bottom face of the concrete slab at the load points. When crushing was first observed at the load points, the crack was generally within $1\frac{1}{2}$ to $2\frac{1}{2}$ inches from the top of the slab. As crushing progressed with increasing deformation, the cracks closed until at unloading, crushing had progressed to the bottom of the slab. In beam CC-4S, considerable shear deformation of the slab at the load points occurred before unloading started as shown in Fig. 7. Similar behavior was generally observed in beams CC-2F and CC-3S except that unloading took place before the slab had crushed to half depth. At the end of the tests large cracks were still present in the lower half of the slab of these two beams. This difference in behavior can be clearly seen in Fig. 7.

6.2 Moment - Curvature Behavior at Plastic Hinge Locations

Two different systems of strain gages were used to measure strains in the steel beams. In beams CC-1F and CC-2F strains were measured at the load points (Sections 1 and 6) at the inflection points (Sections 2 and 5) and over the center support (Sections 3 and 4) with electrical resistance strain gages. (Section locations are shown in Fig. 7 of Ref. 5). Good results were obtained from these gages during the fatigue test program. However at the high strains obtained during the ultimate strength tests, the capacity of these gages was exceeded. Consequently, moments and curvatures during the latter stages of the tests of beams CC-1F and CC-2F could not be computed. To increase the range of strain measurement on beams CC-3S and CC-4S, mechanical gage points were used at the load points (Sections 2 and 6) and over the center support (Section 4). In beams CC-1F and CC-2F bending moments and curvatures were computed from the strains in the steel beam. In beams CC-3S and CC-4S bending moments were computed using a measured reaction at the center support. This reaction was measured with a calibrated compression dynamometer. Curvatures were computed from the mechanical strain gage data.

The moment-curvature results computed from the data thus obtained are summarized in Table 2 and Figs. 9, 10 and 11. Figures 9 and 10 show the moment-curvature behavior at a positive and negative plastic hinge locations for beams CC-1F and CC-2F. Figure 11 shows the same relationship for beam CC-3S. The behavior of beam CC-4S was similar to CC-3S at each plastic hinge location. In these figures the observed start of local flange buckling at the negative plastic hinge location has been shown with an "X". The theoretical moment-curvature curves were based on measured beam properties and an idealized elastic-plastic stress-strain curve.

Although local buckling was observed to start almost simultaneously in the lower (compression) flanges on either side of the interior support of each beam, a major flange buckle would develop only on one side as load was increased. The major flange buckle developed on the west side in beams CC-1F, CC-2F and CC-4S and on the east side in beam CC-3S. Web local buckling was also observed adjacent to each flange buckle. The web buckling extended to nearly the top of the web at each major flange buckle. (Art. 6.1)

6.3 Slip Measurements

Slip measurements were taken at the exterior supports of each beam and at various locations in the negative moment region. Dial gages reading to 0.001-in were used for this purpose.

Previous studies had indicated that if the number of shear connectors provided was adequate to develop the theoretical ultimate bending moment of a cross-section, the load-deflection curve of the member would not be affected significantly by the magnitude of slip.[7] Beams CC-1F and CC-2F had shear connections designed on the basis of the fatigue criteria suggested in Ref. 4 for 2,000,000 cycles of load application. As a result beam CC-1F had 11% and beam CC-2F 12.5% more connectors than would be required for an ultimate strength design using Ref. 4. Beams CC-3S and CC-4S had connectors designed on an ultimate strength basis, but were both fatigued first to 500,000 cycles. Although connector failures had taken place in all four beams during the fatigue tests (see Ref. 5), there was no indication of impending shear failure during the ultimate strength tests.

As was mentioned previously (Ch. 3), the ultimate strength design criteria in Ref. 4 for the design of the shear connection includes a reduction factor of 0.85. On this basis, beams CC-1F, CC-2F, CC-3S and CC-4S each had 29.5%, 32.5%, 17.5% and 17.5% more studs respectively than would be required for static strength if no reduction factor was used.

Table 3 shows the magnitude of slips observed at nine locations in each beam. The slips shown in the Table were measured at the attainment of the maximum load and at the end of the test.

Figures 12 and 13 illustrate the load versus slip behavior at the exterior ends of beams CC-2F and CC-3S. Similar behavior was observed in beams CC-1F and CC-4S. Slip was obtained at each of the interior points where slip measurements were made. Very small slips occurred under the load points as expected. However, over the center support where slip theoretically was zero, appreciable slips were measured as can be seen in Table 3.

6.4 Cracking of Slabs in the Negative Moment Regions

The extent of cracking at the beginning of each ultimate strength test is shown in Fig. 32 of Ref. 5. Additional cracking occurred during each test and cracks widened appreciably as expected. Crack widths were measured on beams CC-3S and CC-4S at the conclusion of the tests using a 40 power microscope.

Figures 14 and 15 show the distribution of cracking throughout the negative moment region of all four beams at the end of the ultimate strength tests. The crack locations were emphasized by painting thin black lines over them resulting in the appearance in the Figures of much wider cracks than actually present.

In beam CC-1F large cracks approximately 6-in to 12-in apart formed throughout the negative moment region. The pattern of cracks was similar to that observed after fatigue testing, but the crack widths were much larger. Additional longitudinal cracks appeared over the center support approximately over the edges of the flanges of the steel beam. A small amount of negative transverse bending was observed over the center support which would account for the presence of these cracks. Although the crack widths were not measured they were estimated to be from 0.10-in to 0.25-in wide based on known crack widths in two of the beams. They were of nearly uniform width across the slab. Since they were of the same magnitude of width throughout the negative moment region, reasonably uniform tensile force existed in this region at the ultimate load. This result was expected as there were no connectors in the negative moment region of beam CC-1F. (Ref. 5).

An entirely different crack pattern is seen in beam CC-2F. One very large crack which measured approximately 3/8 inch to 1/2 inch wide, developed directly over the support. Very little cracking occurred elsewhere as seen in Fig. 14, and was of smaller (0.01-in to 0.10-in estimated) crack width. Most of the cracking occurred within the 22-in length on each side of the center support in which there were no stud connectors (see Ref. 5). Again this was the same pattern that was observed during the fatigue tests except that in those tests the crack widths were much smaller.

The crack patterns of beams CC-1F and CC-2F shown in Fig. 32 of Ref. 5 and Fig. 14 of this report could be expected to occur in present bridge decks where continuous composite bridge girders were designed using the present AASHO Bridge Specifications if the girders were subjected to loads up to the design or to the ultimate load. The particular pattern (CC-1F or CC-2F) would depend on whether or not connectors were placed in the negative moment region.

In beams CC-3S and CC-4S more closely spaced and smaller cracks developed in the slab at the ultimate load. Measured crack widths varied from 0.002-in to 0.26-in in beam CC-3S at the end of testing. In beam CC-4S, the crack widths at the end of testing varied from 0.001-in to 0.21-in. In both beams crack widths were generally less than 0.09-in wide outside a 24-in width directly over the support. Midway between the support and the inflection points the crack widths in both beams were generally less than 0.01-in. Fig. 15 shows the distribution of cracking in beams CC-3S and CC-4S at the end of the static tests.

More pronounced negative transverse bending was observed over the center supports of beams CC-3S and CC-4S. This resulted in increased longitudinal cracking as can be seen in Fig. 15. A short distance from the support these cracks become inclined to between 30^o and 45^o to the longitudinal beam axis. This effect was more pronounced in beam CC-4S. In the immediate vicinity of the center support, vertical shear deformations across the longitudinal and inclined cracks was observed towards the end of testing, especially in beam CC-4S. It can be observed in Fig. 15 that spalling of the slab surface took place about midway between the steel beam and the edge of the slab of beam CC-4S. The spalling took place in the region of the greatest observed shear deformation, and the greatest observed negative transverse bending of the slab.

The location of the spalled surface at the interior support of beam CC-4S is shown again in Fig. 16. It was located approximately at the cross-section containing the center support and lies to the north of the beam axis.

7.0. ANALYSIS OF TEST RESULTS

7.1 Introduction

The concept of plastic design as applied to steel structures is based on the ability of those structures to redistribute internal forces (moments) as yielding takes place in certain regions. Rotation capacity is therefore required at certain potential plastic hinge locations. The ability of steel structures to deform plastically is affected by factors such as (1) moment gradient, (2) spacing of lateral bracing, (3) the end restraint provided by spans adjacent to the inelastic span, (4) the properties of the lateral bracing, (5) the occurrence of local buckling, (6) the material and cross-sectional properties of the beam and (7) the occurrence of lateral torsional buckling.[13] It has been found that for steel structures using wide-flange shapes, lateral-torsional buckling will be the predominant failure mode in uniform moment regions, while local buckling will be the predominant failure mode in regions under moment gradient.[14] Therefore, the properly designed structure must adhere to certain lateral bracing spacing and geometrical restrictions if these failure modes are to be prevented. Composite beams using wide-flange shapes have certain advantages over non-composite beams in that one of the flanges is connected at close intervals to the concrete slab. When this flange is in compression, lateral torsional buckling is prevented by the lateral bracing effect of the slab and local buckling is prevented by the connection to the slab. The connection must of course provide a minimum restraint to prevent such failure modes. Unrestrained (not restrained against lateral torsional and local buckling) flanges in composite beam will be subjected to the same restrictions as wide flange-beams.

In composite bridge girders maximum positive moments are produced by placing the live load on alternate spans. Uniform negative live load moment therefore is produced in the unloaded span. The dead load in this span causes negative moments near the supports and positive moments towards mid-span. If the live load to dead load ratio is sufficiently large, negative total load moments approaching the uniform moment condition, can exist over the entire span. For such a case lateral torsional buckling of the lower (compression) flange is possible. However, this failure mode is unrealistic for practical live load to dead load ratios.

A more realistic failure mode is local buckling of the compression flange of the wide-flange shape near interior supports. Moment gradient exists near the supports of all continuous composite beams and the unrestrained flange is in compression in the vicinity of the interior supports. Therefore, if adequate precautions are not taken, local buckling of either the compression flange or the web can be expected in this region. Lateral restraint from the interior support itself prevents lateral torsional buckling in the immediate vicinity. However, if the negative moment region is sufficiently long and local buckling is prevented, lateral torsional buckling modes remote from the support may be possible and should be investigated.

Composite beams exhibit other modes of failure which cannot occur in non-composite beams. Some of the more important ones (splitting and diagonal tension failure of the slab) were mentioned earlier (Ch. 2).[11,12]

The only secondary failure which occurred during the ultimate strength tests reported in this investigation, was local buckling of the compression flange and web of the wide-flange beam adjacent to the center support. Longitudinal splitting and diagonal tension cracking was observed only in localized regions of beams CC-3S and CC-4S (Fig. 15) and did not affect the beam behavior (Art. 6.4). It is apparent that the longitudinal and transverse reinforcement provided was adequate to prevent this type of secondary failure.

The analysis of the test results presented in Chapter 6 of this report will be confined to (1) the load-deflection behavior and the influence of the observed flange and web local buckling on the load-deflection behavior, (2) the moment-curvature behavior at the plastic hinge locations, (3) the feasibility of applying plastic analysis and ultimate strength theory to the design of continuous composite beams, and (4) the forces on the stud shear connectors and the tensile force in the longitudinal reinforcement.

7.2 Ultimate Strength Behavior of the Continuous Beams

7.2.1 Load - Deflection Behavior

It was evident from Figs. 2 to 5 that the load-deflection behavior of all four beams was similar although there were small differences which will be discussed. It was further evident that three of the four beams (CC-1F, CC-3S, CC-4S) exceeded the ultimate load. (Ch. 4 gives the ultimate flexural capacities). Beam CC-2F reached 97% of the predicted load. All beams exhibited good deformation capacity at their ultimate load.

The load-deflection curves for beams CC-1F and CC-2F (Figs. 2, 3) show a definite bi-linear behavior up to maximum load. In both beams, local buckling was observed to start soon after first yielding and before an apparent negative plastic hinge had developed. (Refer to page 19). First yielding occurred in the compression flange at the center support and spread outwards along the flange. The local flange buckle then developed in the yielded region of each beam. Web buckling also occurred adjacent to the major flange local buckle.

A significant difference in behavior between first yield and the formation of the negative plastic hinge in beams CC-1F and CC-2F can be observed from Figs. 2 and 3. In beam CC-1F, the start of local buckling (point C, Fig. 2) caused no appreciable change in slope. At point B, where the apparent negative plastic hinge developed, the slope changed abruptly especially in the West span. The curve was then approximately linear until crushing of concrete at the load points was observed (point D).

In beam CC-2F, however, the abrupt change in slope of the load-deflection curve (Fig. 3) occurred at or shortly after the start of local buckling (point C). The apparent formation of the negative plastic hinge had little or no effect on the load-deflection curve.

The change in slope of the load-deflection curves for beams CC-1F and CC-2F occurred at approximately the same relative load level and the deflections at this point were nearly the same. It is apparent however, that the change in slope was greater in beam CC-2F than beam CC-1F. Since the start of crushing under the load points was at approximately the same deflection, the result was a lower ultimate load level for beam CC-2F.

Figures 9 and 10 show that a fully effective negative plastic hinge did not form in either beam CC-1F or beam CC-2F. In fact, the negative moment at the support of beam CC-2F (Fig. 10) was erratic and dropped sharply to a low level soon after the theoretical yield moment was reached. In beam CC-1F the moment-curvature behavior was somewhat better (Fig. 9). Although the plastic moment at the support of beam CC-1F was not reached and the moment fell sharply at first, it eventually remained at a nearly constant level(near the theoretical yield moment) for a considerable increase in curvature. This difference in moment-curvature behavior at the negative plastic hinge location partly explains the difference in load-deflection behavior of beams CC-1F and CC-2F.

It is significant to note at this point that even though a fully effective negative plastic hinge did not form (Figs. 9 and 10) in either beam CC-1F or beam CC-2F, the predicted ultimate load capacity was exceeded in beam CC-1F and almost equalled in beam CC-2F. This means then that the theoretical ultimate positive moment of 830 kip. ft. (CC-1F) must have been exceeded. Because the capacity of the electrical resistance strain gages was reached before the ultimate load was attained, the moments at the positive and negative plastic hinge locations of beam CC-1F could not be obtained at the ultimate load.

It was observed however, that yielding had spread to about 4-ft either side of the load points. The stress at the load points was therefore greater than the yield stress. The plastic centroid was in the concrete slab at the initiation of crushing at the load points (observed result). It would be located so that the total compressive concrete force at first crushing would be in equilibrium with the tensile force in the steel beam. Therefore a bending moment greater than the theoretical plastic moment of the section could have developed at the ultimate load due to strain hardening. A further substantiation of this argument will now be discussed.

Tests of two simple span composite beams (designated beams SC-1S and SC-2S) were reported in Ref. 20. The cross-sections of these beams were nearly identical to the cross-sections at the load points of the four continuous composite beams reported herein. The material properties varied slightly however between the 6 beams. Beams SC-2S and CC-1F were tested to ultimate load at approximately the same time. The computed ultimate moment capacity of beam SC-2S was 742 k-ft. The experimental ultimate moment capacity was 850 k-ft which exceeded the computed value by 14.5%. On this basis it would be reasonable to assume that the theoretical ultimate positive moment capacity of beam CC-1F could also have been exceeded by a similar amount.

Figures 4 and 5 show load-deflection curves for beams CC-3S and CC-4S which are somewhat different than those for beams CC-1F and CC-2F (Figs. 2 and 3). The transition from the start of yielding (point A) to the formation of the negative plastic hinge (point B) and beyond to the ultimate load capacity was more gradual. This is the characteristic behavior of a composite beam in the absence of secondary failures. The start of local buckling (point C) had no appreciable effect at that point on the load-deflection behavior of beam CC-3S (Fig. 4). For beam CC-4S, local buckling occurred almost at the predicted ultimate load and caused a levelling off of the load-deflection curve. It is quite apparent that the introduction of stiffeners near the center support of these two beams greatly improved their load-deflection behavior.

The moment-curvature behavior at the negative plastic hinge location of beams CC-3S and CC-4S was also improved. The negative moment in beam CC-3S reached 94% of the theoretical plastic moment and remained relatively constant for a large increase in curvature, (Fig. 11 and Table 2).

A similar behavior was obtained for beam CC-4S although the maximum negative moment ratio was slightly smaller (Table 2).

A similar argument to that used previously for beams CC-1F and CC-2F explains why the ultimate loads of beams CC-3S and CC-4S were also reached when the negative plastic hinge did not quite develop. It can be concluded that the ultimate positive moment capacity of these two beams also was exceeded due to strain hardening. Figure 7 shows the spread of yielding at the load points of beams CC-3S and CC-4S.

In beams CC-1F and CC-2F, strain data was obtained from the electrical resistance strain gages up to and somewhat beyond the occurrence of buckling. However, moment-curvature data was obtained up to the end of testing at the plastic hinge locations in beams CC-3S and CC-4S. It is apparent from Fig. 11 that the positive plastic hinge moment of 770 k-ft was exceeded in beam CC-3S. It was also exceeded in beam CC-4S. Since the cross-sections at positive plastic hinge locations of all four beams was identical it is also reasonable to assume that the positive plastic moment was also exceeded in beams CC-1F and CC-2F as previously discussed. Large curvatures were associated with the attainment of the plastic moment at positive hinge locations in beams CC-3S and CC-4S. Because of the greater degree of interaction in beams CC-1F and CC-2F (depending of course on the number of failed studs in each beam) it is also reasonable to assume that the plastic moment would be reached at slightly smaller curvatures. Some indication of the relative degree of interaction between the four beams can be obtained from Table 3 and

Figs. 12 and 13. The slips in beams CC-1F and CC-2F were generally smaller than the slips in beams CC-3S and CC-4S.

7.2.2 Local Buckling

Because of the flange and web buckling which occurred at the interior support of the four continuous beams (Fig. 6) a preliminary study will be made in this article in an attempt to determine the probable cause. The results should be useful when designs are made for future continuous composite beam tests where buckling failures must be avoided. The discussion will center on the width-thickness requirements of the flange and web of the 21W62 section adjacent to the center support.

(1) Flange and Web Local Buckling - Flexure

Lay and Galambos,[14,15] discuss the inelastic behavior of wide-flange beams under moment gradient. Further discussion is given in Ref. 16 and tentative recommendations for local buckling of wide flange shapes are given in Ref. 17.

The problem analyzed by Lay was the minimum required width-thickness ratio of a compression flange which will allow average strains equal to the attainment of the strain-hardening strain before local buckling begins. The material properties used in the analysis were those corresponding to the on set of strain-hardening.

Lay found the critical width-thickness ratios for the compression flange by solving the torsional buckling problem. Solutions for two cases were presented; the first gave the limiting width-thickness ratio assuming that the fully yielded flange was subjected to a uniform compressive stress equal to the yield stress level of the flange material (uniform moment) while the second was presented for the case of a compression flange under moment gradient, where the strains were above the strain-hardening strain. Therefore in this case the stress was greater than the yield stress level. Using typical properties for A36 wide-flange shapes[17] the width-thickness limitations were found to be 18.4 (uniform moment) and 17 (moment gradient). The small (3%) contribution of the web restraint was neglected in each case.

It should be pointed out that the equations for the width-thickness ratios derived in Ref. 14 should be applicable to the unrestrained (unrestrained from local buckling) compression flange of a wide-flange shape used in composite beams since the problem is similar to local buckling in ordinary wide-flange shapes.

Lay and Galambos point out in Refs. 14 and 15 that for the moment gradient case, the yielded zone is concentrated into a restricted region. The criterion then is that local buckling can only occur when the yielded length equals the full length of a potential local buckle. The length required for a potential locak buckle is dependent on material and geometry but independent of span length and moment gradient. However, the actual yielded length of a flange will be dependent on the value of moment at which the flange begins to yield and the form of the bending moment diagram.[14]

Table 4 shows the actual width-thickness ratios of the compression flange of the 21W62 section near the center support of each of the four continuous composite beams. The depth-thickness ratios of the web are also shown. These values were computed from the measured dimensions of the wide-flange beams which are contained in Table 5 of Ref. 5.

Table 4 also shows the required yielded length of the compression flange to develop a potential local buckle and the computed yield length at the attainment of the full positive and negative plastic hinges (mechanism) in each beam. For beams CC-3S and CC-4S the required length for a potential local buckle was based on an unrestrained flange (no stiffeners).

The allowable width-thickness ratio for the flange and the allowable depth-thickness ratio for the web of a rolled wide-flange shape which have been taken from Ref. 18 are shown below Table 4. The value of 17.5 for the flanges includes the 3% increase for the web contribution. This assumes that a section under uniform compression can be strained to the point of strain-hardening before local buckling influences its carrying capacity.[19] The value of 70 for the web assumes bending with zero axial load. Both of these ratios were derived for symmetrical I, W or H shapes used as beams or columns.[19]

The actual material properties of the wide-flange beams differed somewhat from those assumed in the derivation of the preceeding allowable width-thickness and depth-thickness ratios.[5,17] Using the actual values of tensile strength and static yield stress for the flange material, and the values of the modulus of elasticity and the strain hardening modulus, all given in Table 3 of Ref. 5 the following ratios are obtained:[17]

Allowable width-thickness ratio of flange - 15.2

Allowable depth-thickness ratio of web - 71.7

Although the flange and web of the wide-flange shapes used in the four continuous composite beams appeared to be adequate against local buckling based on the limitations of Ref. 18, the adequacy of the flanges apparently was only marginal when based on the actual material properties. It is evident then that local buckling of the flange could be expected to occur. In fact, for beams CC-1F and CC-2F flange buckling did occur soon after first yielding over the center support (Figs. 9 and 10) and considerably before the attainment of the theoretical fully yielded lengths required to develop a local buckle in the compression flange.

The slightly improved behavior of beam CC-1F over beam CC-2F can be partly explained on the basis of three factors, (1) differences in geometry; CC-1F had a smaller flange width-thickness ratio, (2) differences in material properties, and (3) greater flange restraint at the center support of beam CC-1F; for beam CC-1F the flange rested directly on a steel bearing plate whereas 3/8-in of lead fillers separated the flange and the bearing plate of beam CC-2F. (See Ref. 5). During fatigue testing, the lead fillers at the interior bearing of beam CC-2F developed a rounded surface in the longitudinal direction thus moving the boundary of a potential buckled length nearer to the center of bearing. It is probable that the lead fillers developed a rounded surface in the transverse direction also. This would tend to decrease the flange restraint at the point of bearing.

However, even with these minor differences the behavior of both beams CC-1F and CC-2F with respect to buckling was very poor.

It is apparent from the test results that the buckling behavior of beams CC-3S and CC-4S was much improved. This was due no doubt to the presence of the stiffeners. If the stiffeners had not been provided, earlier local buckling and poorer behavior could have been expected because the flange width-thickness ratios of these two beams were greater than in beams CC-1F and CC-2F.

Two observations concerning the observed local buckling should be stressed at this point. First, there was no sudden unloading of the test beams at local buckling. In fact, in all cases, load either increased further or stabilized after local buckling. It is evident that post-buckling strength was available. These tests provide additional experimental verification of the statement in Ref. 15, "There is no reason why local buckling in a cross-section would cause unloading of the member". Secondly, the plastic hinge capacity at the interior support of <u>these test beams</u> does not greatly affect the ultimate load capacity of the beam (Tables 1 and 2). A 45% increase in the computed negative plastic moment (508 to 737 k-ft) results in only a 10.8% increase in ultimate load capacity (172.4 to 185.8 kip). Therefore a significant reduction in negative moment due to buckling would not be expected to greatly affect the load carrying capacity. This may not be true of haunched beams, or of negative moment sections which have cover plates on the compression flange to control the locations of the neutral axis and plastic centroid.

At this point it appears that the webs of all four continuous composite beams were adequate and that the local buckling which occurred was due to too high values of width-thickness ratios of the flanges. However, the computed value of allowable depth-thickness ratio for the webs (71.7) was based on bending only. The possible reduction due to shear and axial forces should be investigated.

(2) Web Local Buckling - Shear

The maximum shear force on either side of the center support did not exceed 105 kips in any test. Using this value of shear, Section 2.4 of Ref. 18 gives a required shear capacity of the web (kips) at ultimate load, of 20.5 times the web area (in^2). The measured yield stress level of the web was used in this derivation (Ref. 5). Based on the measured web thickness (Ref. 5) the minimum required depth-thickness ratio of the web will then be 28. This is considerably less than the actual values (Table 4). Adequate web area was therefore provided on this basis to resist the maximum shear force. However, the validity of this analysis must be viewed with the understanding that the equation in Ref. 18 was derived for a rectangular element in a symmetrical H, W or I shape.[19]

(3) Web Local Buckling - Flexure and Axial Force

In the negative moment regions of continuous composite beams, the force in the longitudinal slab reinforcement introduces compressive forces to the steel beam through the shear connectors. If shear connectors are not present in the negative moment region compressive forces are introduced near the inflection points providing the longitudinal reinforcement is adequately anchored at these points.

In beam CC-1F, with no connectors in the negative moment regions, relatively uniform compression exists over the entire negative moment region (See Fig. 39 of Ref. 5). In beam CC-2F, a nearly uniform compression would exist in a 44-in length over the center support since there were no connectors in this region. Similarly, in beams CC-3S and CC-4S where this length was reduced to 20-in and 12-in respectively (Fig. 4, Ref. 5). Because uniform compression would also exist between the connectors, and the reduction at each line of connectors is relatively small, approximately uniform compression would exist over longer lengths than those stated above.

The maximum value (neglecting strain hardening) of this compressive force can be taken as the area of longitudinal reinforcement times its yield stress level or the yield force level of the steel beam whichever is smaller. On this basis, the compressive forces developed at the interior supports of beams CC-1F, CC-2F, CC-3S and CC-4S would be 110, 110, 317 and 675 kips respectively. Using the requirements of

Ref. 18 for combined axial force and plastic bending moment at ultimate loading, the maximum depth-thickness limitations of the webs of beams CC-1F, CC-2F, CC-3S and CC-4S are 54, 54, 43 and 43 respectively (where 43 is the minimum required). On this basis, beams CC-1F and CC-2F appear to be satisfactory but beams CC-3S and CC-4S do require web stiffeners, (Table 4). Web stiffeners were provided adjacent to the center support of these two beams but apparently were spaced too far apart since buckling did occur. The spacing of the web stiffeners was chosen to suit the spacing of the finger plates which provided lateral and longitudinal stability during the fatigue tests (Ref. 5).

As pointed out earlier, beams CC-1F and CC-2F buckled approximately at the first yield load and considerably before ultimate load. Assuming that no interaction occurred in a small length over the support (44-in in beam CC-2F) the compressive force on the steel beams can be determined from the measured strains at sections 3 and 4 which were within this length, (Ref. 5). On this basis the compressive force was 134 kips (approximately the same for both beams) and the required depth-thickness ratio was 50. This is only slightly greater than the measured values shown in Table 4. The value of 134 kips was a measured value and exceeds the value of 110 kips stated previously due to strain hardening.

It must again be pointed out that the limitations provided in the specifications[18] have been based on symmetrical H, W or I shapes.[19] Furthermore, it was assumed that the total section area was equal to twice the web area and that the maximum strain was four times the yield strain. Although the first assumption is approximately satisfied, higher strain levels could be expected in the steel section of continuous composite beams. However, if these considerations are conveniently ignored, it is apparent from this discussion that web buckling due to flexure and axial force was also a major factor contributing to the local buckling which was observed in the continuous composite beam tests.

(4) Summary

Although this analysis of local buckling has been preliminary in nature, it does serve to indicate that in these tests (1) flange and web local buckling could have been expected to occur in an unrestrained section near the center support, (2) flange local buckling occurred earlier than expected because of the difference in material properties, and (3) web local buckling was influenced by the axial force introduced by the shear connectors. Additional research is required to establish design rules which will allow the full negative plastic hinge to develop in singly symmetric and unsymmetric continuous beams prior to flange and web local buckling.

No local buckling of the steel beam was observed in the positive moment regions during the continuous beam tests, even though the top flange at the load points of beams CC-1F and CC-4S was under compression (Art. 6.1). Local buckling of the wide-flange beam in this region was, however, observed during the test of beam SC-1S which was reported in Ref. 20. This difference in behavior can be attributed to (1) the difference in strain levels, and (2) the difference in stud connector spacing.

7.3 Feasibility of Plastic Design of Continuous Composite Beams

On the basis of this investigation it can be concluded that if the negative plastic hinges are allowed to form first, continuous composite beams can be designed by plastic analysis. It was apparent from the test results that even with serious local buckling at the interior support, the load predicted by the simple plastic theory was exceeded in three of the four tests. The remaining beam (CC-2F) reached 97% of the predicted load.

In a sense, the local buckle in the three successful tests took the place of the negative plastic hinge. As buckling developed the moments remained fairly constant (Figs. 9 and 11), as would be required of a plastic hinge, although at a lower level than the theoretical negative plastic hinge moment. In the remaining test, (CC-2F) the value of moment was not constant after local buckling occurred (Fig. 10).

It is further apparent from these test results that even in the absence of local buckling it would not have been possible to provide sufficient longitudinal reinforcing steel in the negative moment region to cause the positive plastic hinge to form first. To accomplish this would have required either a reduction of the slab width at the load points, an increase in beam depth at the interior support (haunch) or a cover plate on the compression flange at the interior support. The longitudinal reinforcement in beam CC-4S was designed so that the three plastic hinges would form at the same load (based on assumed properties). However, the measured and assumed properties were sufficiently different that this was not possible (Fig. 3, Ref. 5).

7.4 Forces on Stud Connectors

It was of interest to examine the maximum forces to which the shear connectors were subjected during the ultimate strength tests. The previous fatigue tests (Ref. 5) had resulted in almost complete failure of bond between the steel beam and the concrete slab in each composite beam. As a result, the slab force had to be resisted by the connectors alone. Only directly under the load points was bond not broken during the fatigue tests.

As previously mentioned, the high strains in the wide-flange beam which were associated with the ultimate load, exceeded the capacity of the electrical resistance strain gages attached to beams CC-1F and CC-2F. Therefore, in the absence of mechanical gage points no data was obtained from which slab forces could be computed.

However, slab forces were computed from strain measurements on the wide-flange shapes of beams CC-3S and CC-4S. Strain data from the electrical resistance strain gages at sections 1, 3, 5 and 7 (Ref. 5) and from the mechanical strain gage points at sections 2 and 6 was used. Due to the severe local buckling of the wide-flange beam, slab forces at section 4 computed from the mechanical strain gage data at that section were not reliable.

Fig. 17 compares the design cumulative resistance of the shear connectors in beams CC-3S and CC-4S with the force in the slab computed from the strains at the aforementioned sections along the beam. The maximum value of the slab force at each section is shown. This did not necessarily occur at the same value of loading. Generally, however, the maximum slab force occurred either at or following the first attainment of the ultimate load. The design cumulative resistance (stepped curves) was based on an ultimate strength of 31.0 kips per 3/4-in stud shear connector as given in Ref. 7 (3,500 psi concrete strength). Since the deign includes a reduction factor of 0.85 it was expected that the test points would fall somewhat lower than the design curves.

The slab forces in beam CC-3S are lower than in beam CC-4S in the positive moment regions even though the ultimate loads of the two beams were approximately equal. The reason for this was contained in an earlier observation. Beam CC-3S began to unload as crushing of the slab began. Therefore since only part of the slab depth was at the crushing stress, a smaller force existed in the slab (Fig. 7). On the other hand, crushing progressed through the entire depth of beam CC-4S before unloading began. As a result, the slab force was higher (Fig. 7).

The slab force at sections 3 and 5 of beam CC-3S was also lower than in beam CC-4S.

7.5 Force in the Longitudinal Slab Reinforcement

Figure 17 shows the maximum total force in the longitudinal slab reinforcement at section 4 of beams CC-3S and CC-4S. In each case the force shown occurred approximately at the ultimate load. Since the concrete at this section was cracked the force in the reinforcement represents the total slab force. Good agreement exists between the value of this force and the cumulative resistance of the shear connectors.

7.6 Comparison of Beam Performance

The major variable in these tests was the percentage of longitudinal reinforcement at the negative plastic hinge location of each continuous beam. Beams CC-1F and CC-2F each had 2.20-in^2 (0.61%). Beam CC-3S had 7.04-in^2 (1.96%) and beam CC-4S had 16.20-in^2 (4.50%). (Refer to Fig.2, Ref. 5). The longitudinal reinforcement (2.20-in^2, 0.61%) at the positive plastic hinge location of each beam was held constant.

The behavior of each beam was masked to some extent by the occurrence of local buckling at the interior support. However, in beams CC-3S and CC-4S the stiffeners provided near the interior support, controlled buckling to the extent that the behavior of these beams was nearly that which would have been expected had buckling not occurred. The behavior of beams CC-1F and CC-2F was poorer but was remarkedly good considering the severity of buckling which did occur.

The prior fatigue tests of the four beams had no deterimental effect on the ultimate strength behavior, even though considerable fatigue failures occurred in the stud shear connection. On the basis of these tests it can be concluded that the shear connection of continuous composite beams designed in accordance with the recommendations of Ref. 4 will have sufficient strength to develop the ultimate flexural strength of the member. Furthermore, it can be expected that the collapse mechanism can be developed.

The pattern of slab cracking in each beam differed appreciably. The crack pattern of beam CC-2F at the ultimate load was the least desirable, and was apparently due to (1) the long interval over the center support (44-in) in which no shear connectors were provided and (2) the lower percentage of longitudinal reinforcement (0.61%). The crack patterns of beams CC-3S and CC-4S were more desirable. However, the large increase in reinforcement in beam CC-4S provided little improvement in slab crack behavior over beam CC-3S.

7.7 Variables Requiring Further Study

(1) The fatigue tests reported in Ref. 5 suggested that the spacing of connectors and the amount of longitudinal reinforcement in the negative moment region of continuous composite beams required additional study. That work was considered necessary in view of the fatigue requirements of the steel beam, and to establish criteria for optimum

crack control of the concrete slab. When considering these variables from this point of view, attention should also be given to the moment-curvature behavior at the potential negative plastic hinge location, especially following the minimum number of cycles of load application chosen in the fatigue studies. This work is required to ensure adequate rotation capacity of the negative plastic hinge. This relationship could not be studied conclusively in the ultimate strength tests reported herein because of premature local buckling.

(2) This investigation has shown that a detailed study of local buckling of continuous composite beams is required. This study should follow studies already made on flange and web buckling of symmetrical I, W and H shapes but should be specifically orientated towards singly symmetric composite steel-concrete beams using wide-flange shapes. Consideration should be given to the placement of shear connectors and the degree of interaction in the negative moment region. When the significant parameters have been established design rules for the economical control of buckling should be developed. An extension of this work to the buckling of non-symmetric composite steel-concrete beams should also be made.

(3) In haunched continuous composite bridge girders an ultimate strength design could be attempted where the positive plastic hinges form first. A similar situation could arise if cover plates are

used on the compression flange at the interior supports. Further tests are required to investigate the feasibility of plastic design for such cases and possibly to establish slab reinforcement requirements at the positive plastic hinge locations to ensure adequate rotation capacity of these hinges.

(4) Ultimate strength tests should be carried out in conjunction with the further fatigue investigations suggested in Ref. 5 to determine the effect of slab width-thickness ratios and prestressing on the moment-curvature behavior at negative plastic hinge locations.

8.0 SUMMARY

The results of ultimate strength tests of four continuous composite steel-concrete beams has been presented in this report. Each beam had two equal spans of 25 feet and consisted of a 60 inch wide by 6 inch reinforced concrete slab connected to a 21W62 A36 steel beam with 3/4 inch diameter by 4 inch high headed steel stud shear connectors. Each continuous composite beam had been subjected to fatigue tests prior to the ultimate strength tests. The fatigue test program was discussed in Ref. 5.

The purpose of the ultimate strength tests was two-fold: (1) to determine if sufficient shear capacity remained to develop the flexural strength of the beam and (2) to further investigate the feasibility of applying the concepts of plastic analysis and ultimate strength theory to the design of continuous composite beams.

The following conclusions were drawn from an analysis of the test results:

(1) Shear connectors designed on the basis of the static and fatigue requirements contained in Ref. 4 will provide sufficient shear connection to develop the ultimate flexural strength of the member after the design cycle life of the connection in fatigue has been reached.

(2) On the basis of this investigation, plastic analysis and ultimate strength theory can be used for the design of continuous composite beams.

(3) The tensile strength of the longitudinal reinforcement in the slab can be used in the design.

(4) Local flange and web buckling near the interior supports of continuous composite beams limits the ultimate load capacity of the member; further analytical and experimental studies are required to establish design rules which would allow the full negative plastic hinge to develop prior to flange and web local buckling.

(5) Further studies are required to establish the rotation capacity of negative plastic hinges.

(6) Tests of continuous composite beams are required in which the positive plastic hinges are the first to form.

9.0 ACKNOWLEDGMENTS

The study described in this report was part of an investigation on composite beams that was conducted at Fritz Engineering Laboratory, Department of Civil Engineering, Lehigh University. L. S. Beedle is Acting Chairman of the Department and Director of the Laboratory. The project was financed by the New York Department of Public Works, the Department of Commerce - Bureau of Public Roads, Nelson Stud Division of Gregory Industries, Inc., KSM Products Division of Omark Industries Inc., Tru-Weld Division of Tru-Fit Screw Products Inc., and Lehigh University.

The writers wish to thank Dr. R. G. Slutter for his advice and help in the planning and conduct of these tests. Sincere thanks are also due Noriaki Yoshida for his assistance in the conduct of several of the tests and for his aid in reducing and analyzing the test data: to Messrs K. R. Harpel and C. F. Hittinger and their staff at the Fritz Laboratory for their work in preparing the test set-up and instrumentation; to R. N. Sopko and his staff for preparing drawings and providing the photographic coverage; and to Mrs. D. Eversley for typing the manuscript.

10.0 TABLES AND FIGURES

TABLE 1

RESULTS OF TESTS ON CONTINUOUS BEAMS

Beam No.	LOAD (KIPS)				DEFLECTION (IN.)			
	FIRST YIELD		MAXIMUM		WEST LOAD POINT		EAST LOAD POINT	
	Theor.	Test*	Theor.	Test	At Maximum Load	End Of Test	At Maximum Load	End Of Test
CC-1F	125.0	115-125	172.4	180.0	3.81	6.91	5.00	8.07
CC-2F	128.0	115-125	177.6	173.0	4.86	8.47	4.62	6.62
CC-3S	131.5	115-125	178.2	191.0	5.55	7.45	5.66	7.55
CC-4S	126.0	115-125	185.8	192.0	3.91	9.88	4.10	10.59

* Definite first yielding was difficult to assess due to residual stress condition near welds. However considerable yielding was observed to start at the centre support of each beam between 115 and 125 kips.

TABLE 2

MOMENT-CURVATURE BEHAVIOR AT NEGATIVE PLASTIC HINGE LOCATIONS

Beam No.	THEORETICAL RESULTS					TEST RESULTS		
	At First Yield			Plastic Hinge Moment	Ratio of Plastic Hinge Moment to yield Moment	At Flange Buckling		Ratio of Bending Moment at Flange Buckling to Plastic Hinge Moment.
	Curvature	Bending Moment	Load			Curvature	Maximum Bending Moment	
	X10-6 Rad./in.	k-ft	k	k-ft		X10-6 Rad./in.	k-ft	
CC-1F	77.0	327.0*	125.0	508*	1.555	103.8	435.0	0.855
CC-2F	77.0	327.0	128.0	508	1.555	82.0	400.6	0.789
CC-3S	73.0	408.0	131.5	633	1.550	507.7	595.0	0.940
CC-4S	61.5	445.0	126.0	737	1.656	601.0	665.0	0.902

* Longitudinal Reinforcement was considered when computing the yield and plastic moments

** The onset of flange buckling was determined by visual observations and by examination of strain data near the buckle.

TABLE 3

MAGNITUDE OF SLIPS AT MAXIMUM LOAD AND AT END OF TEST-IN INCHES

BEAM NO.	WEST SPAN								CENTER		EAST SPAN							
	A		B		C		D		E		F		G		H		I	
	MAX*	END**	MAX	END	MAX	END	MAX	END	MAX	END	MAX	END	MAX	END	MAX	END	MAX	END
CC-1F	.017	.029	--	--	.116	.210	.144	.217	.044	.016	--	--	.193	.292	--	--	.013	.019
CC-2F	.018	.023	.020	.044	.024	.032	.017	.024	--	--	.019	.028	.023	.028	.005	.004	.013	.019
CC-3S	.052	.076	.109	.144	.106	.234	.103	.230	.058	.110	.111	.190	.126	.216	.134	.219	.059	.075
CC-4S	.068	.249	.078	.127	.064	.110	.060	.196	.009	.049	.045	.065	.058	.081	.064	.089	.058	.128

* Slip corresponding to the maximum test load

** Slip corresponding to the load at the end of the test

TABLE 4

LOCAL BUCKLING

BEAM NO.	Width (Depth) - Thickness Ratios for 21W62		Required Length for a Flange Local Buckle	Yielded Length at the Formation of a Mechanism
	FLANGE*	WEB**		
CC-1F	13.85	48.00	18.58	14.80
CC-2F	14.30	47.80	18.20	13.70
CC-3S	14.75	48.40	17.90	19.40
CC-4S	14.60	49.00	17.90	20.40

* Allowable width - thickness ratio for flanges of rolled shapes is 17.5 (Ref. 18)

** Allowable depth - thickness ratio for webs of rolled shapes (bending) is 70. (Ref. 18). For combined bending and axial force this value is to be reduced by 100 times the axial load ratio (axial force / yield force).

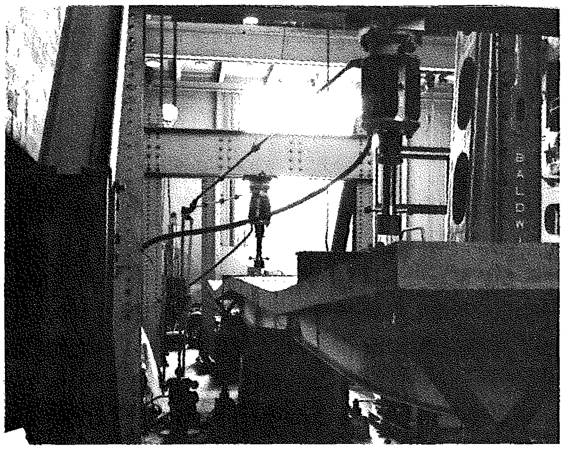

CC-1F

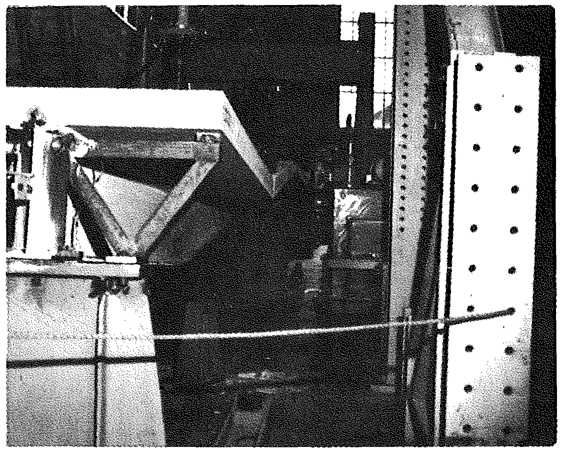

CC-2F

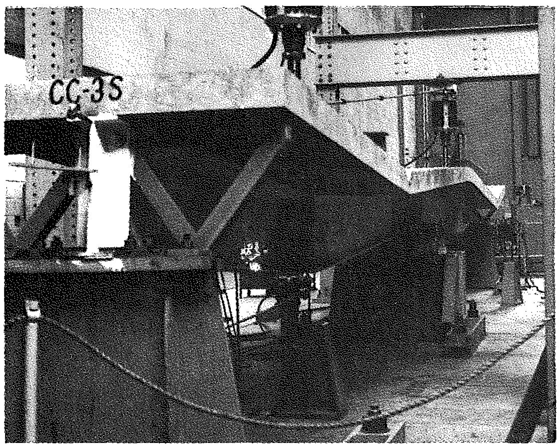

CC-3S

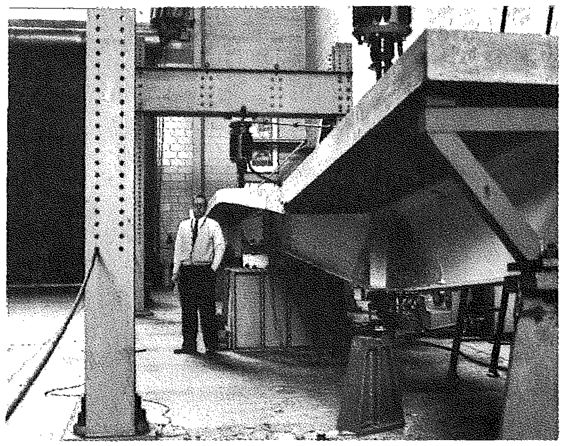

CC-4S

FIG. 1 - STATIC TESTS OF THE CONTINUOUS COMPOSITE BEAMS

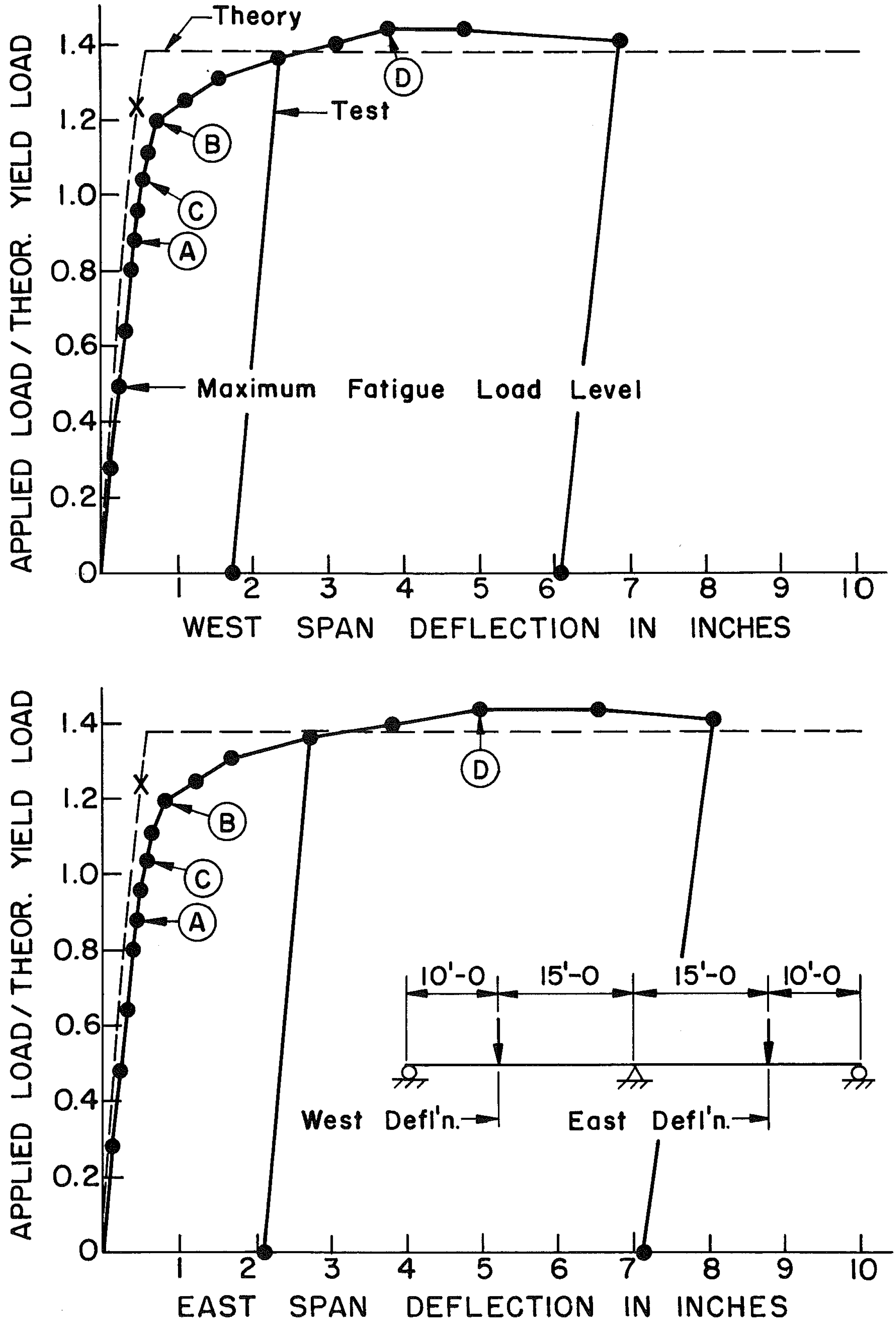

FIG. 2 - CC-1F LOAD - DEFLECTION CURVES

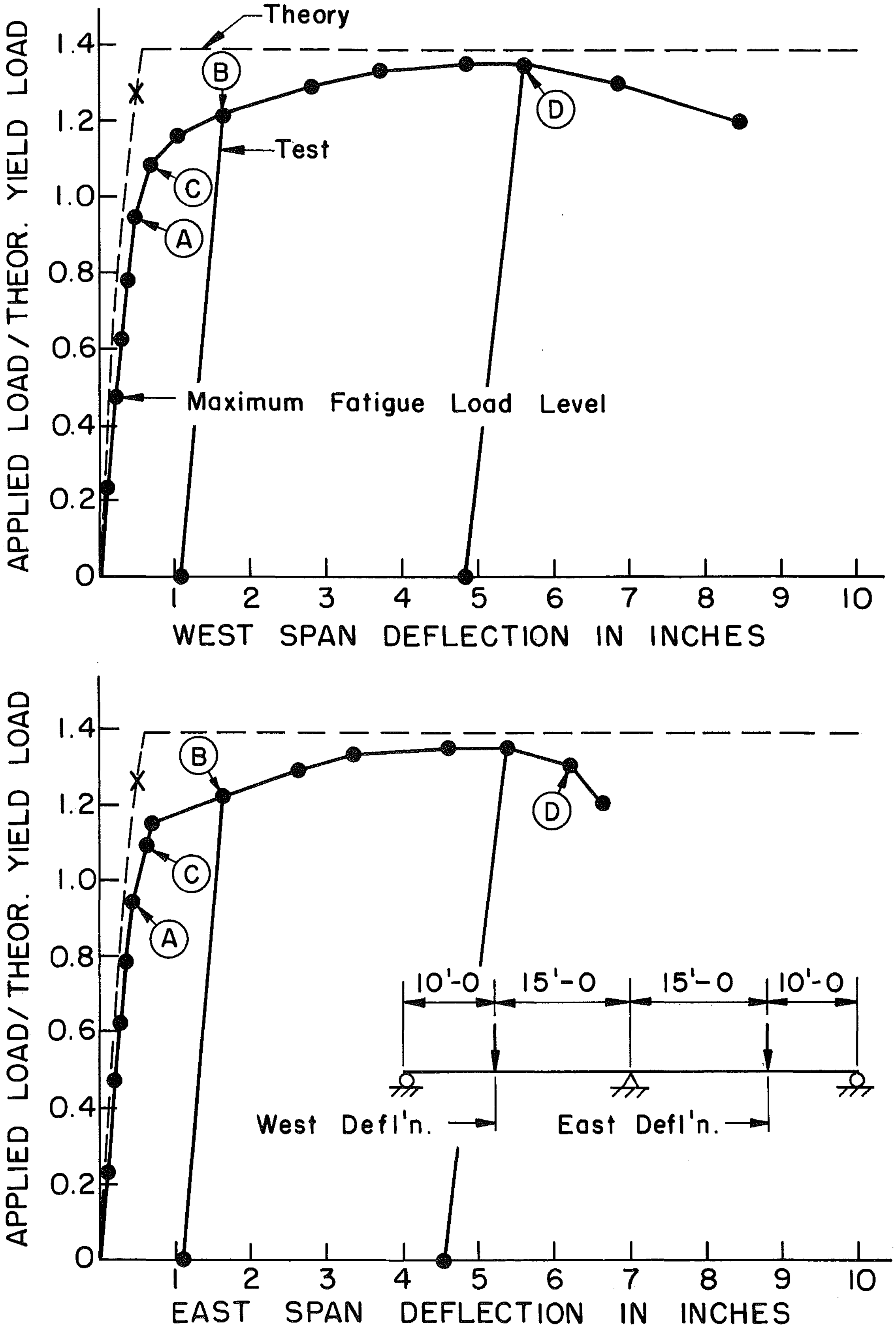

FIG. 3 - CC-2F LOAD - DEFLECTION CURVES

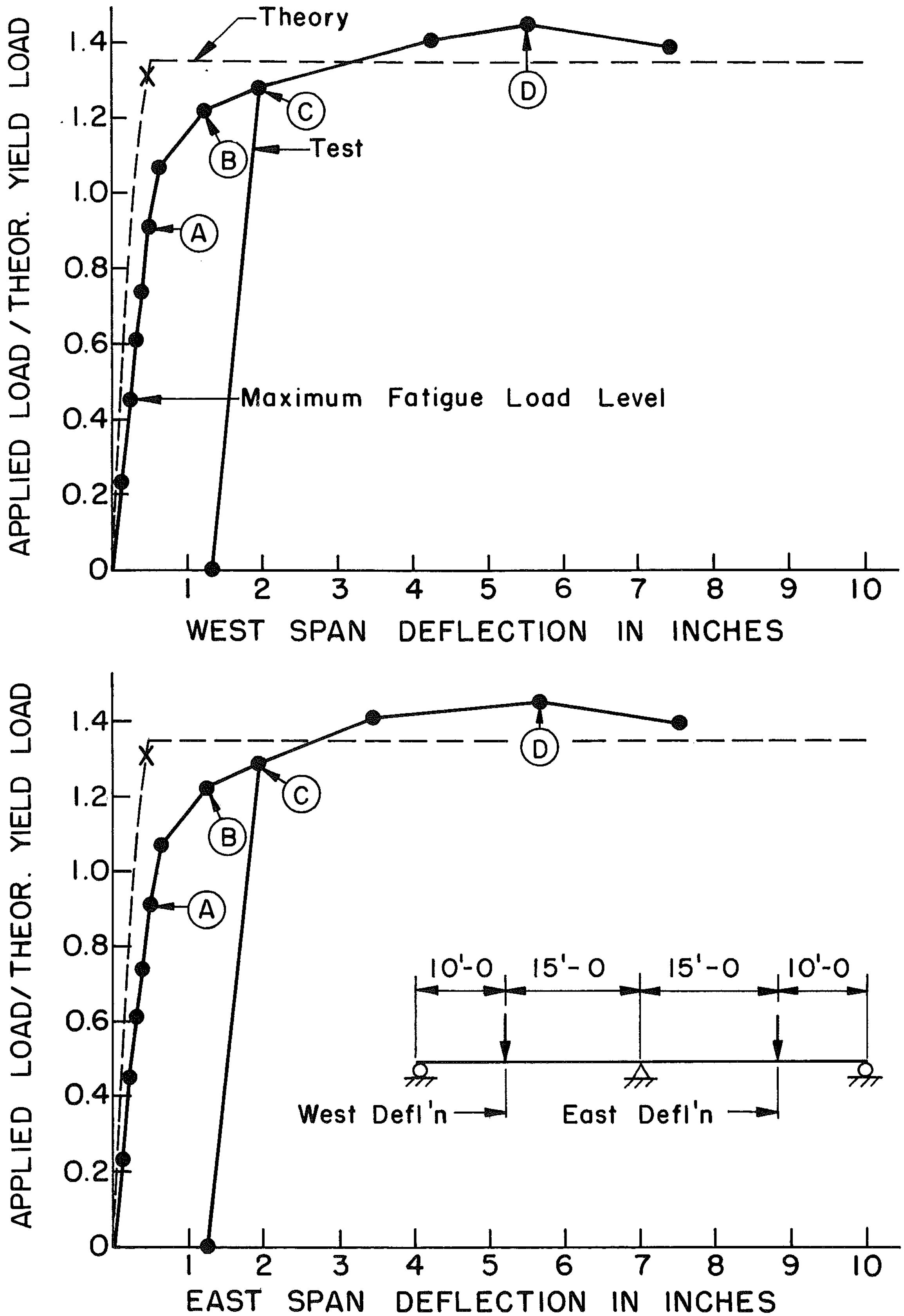

FIG. 4 - CC-3S LOAD - DEFLECTION CURVES

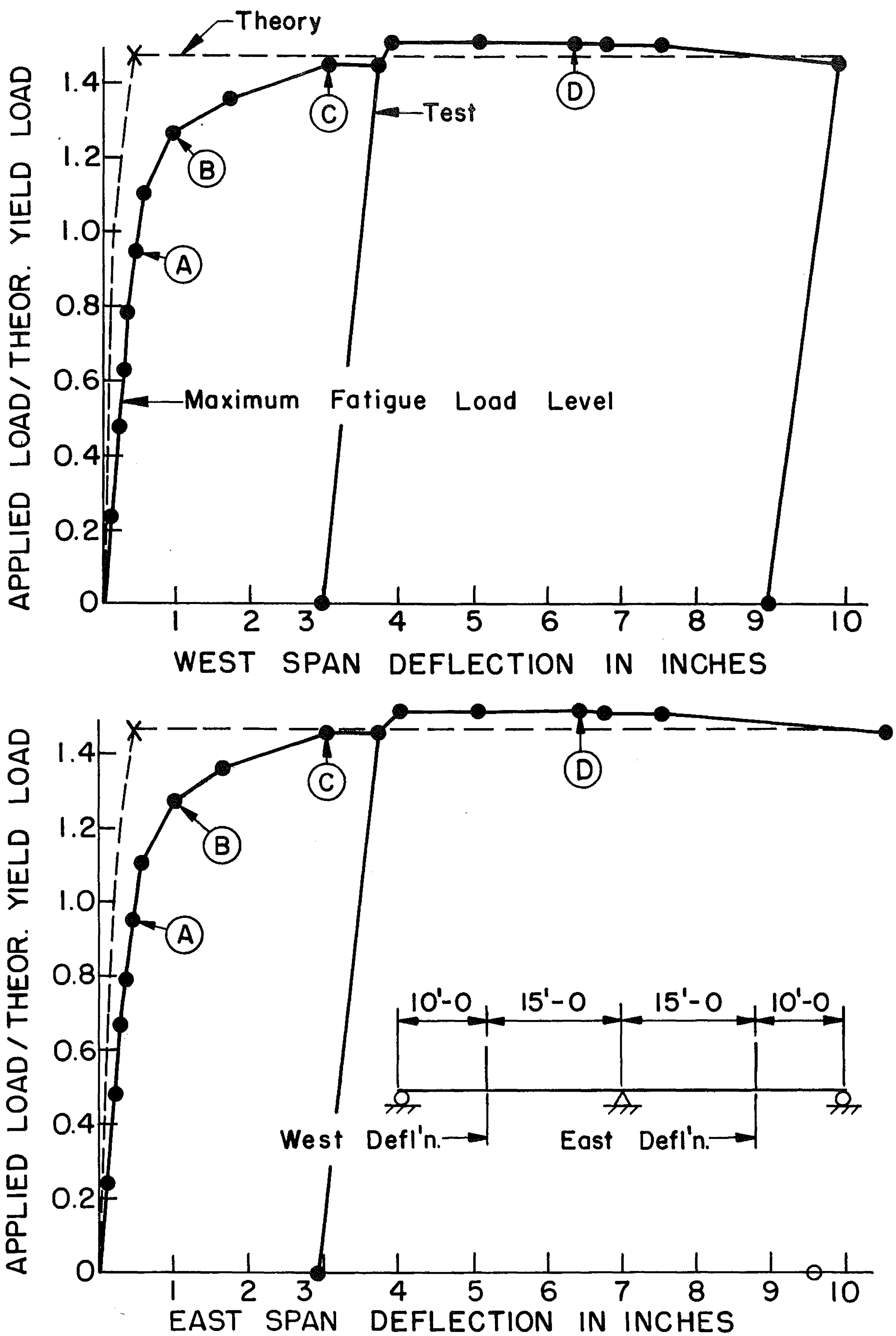

FIG. 5 - CC-4S LOAD - DEFLECTION CURVES

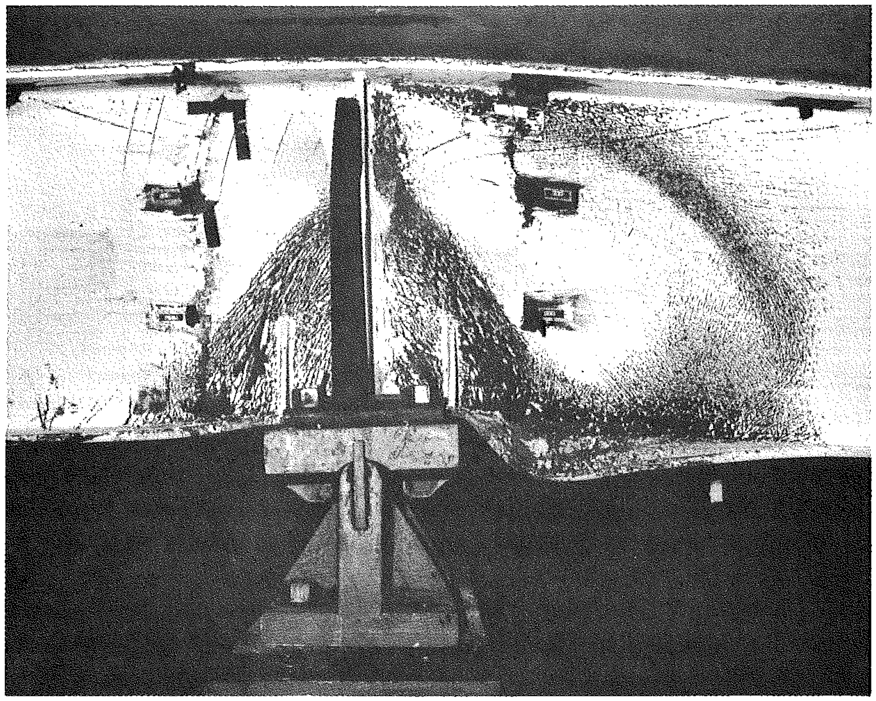

CC-2F

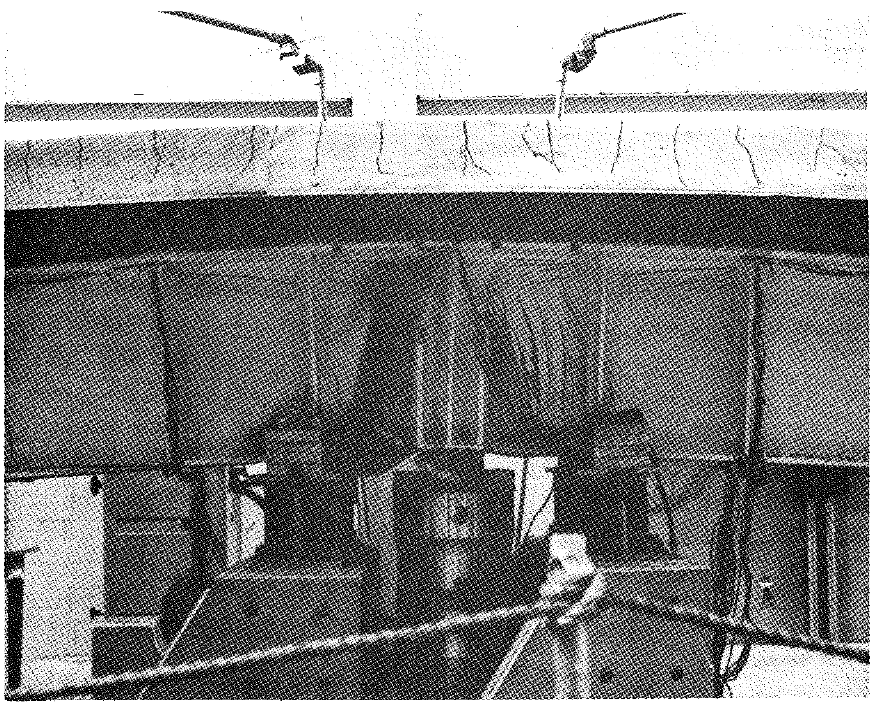

CC-4S

FIG. 6 - TYPICAL LOCAL FLANGE AND WEB BUCKLING

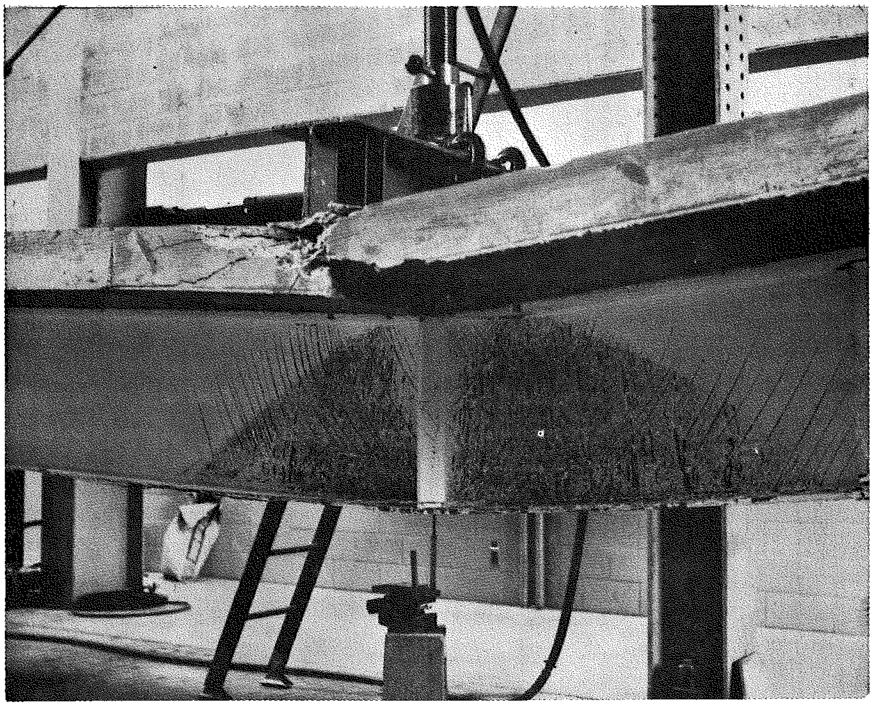

CC-4S

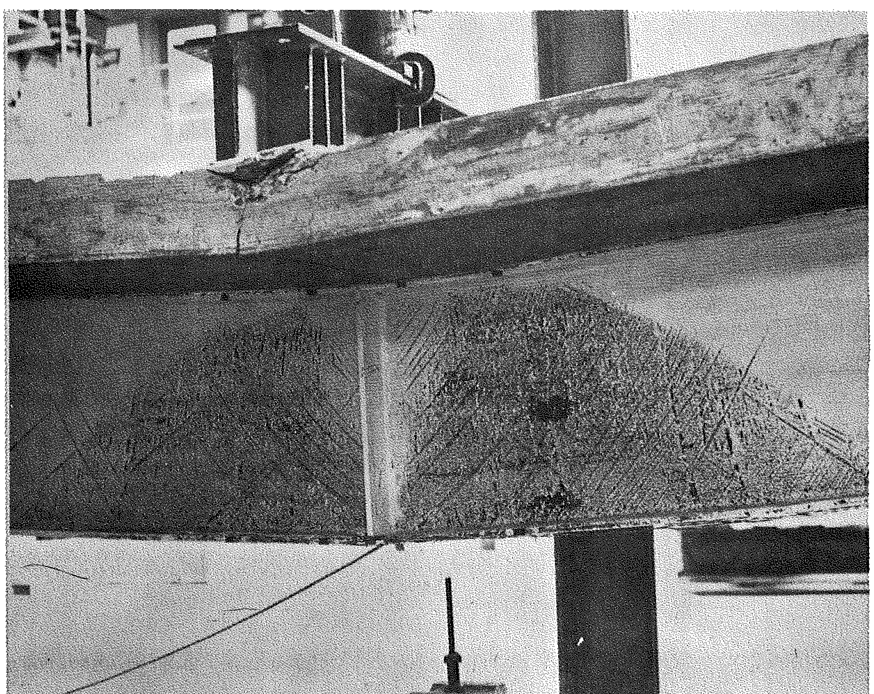

CC-3S

FIG. 7 - CRUSHING OF SLAB AT LOAD POINTS

CC-4S

FIG. 8 - CRUSHING ON LOWER SLAB FACE OVER THE CENTER SUPPORT

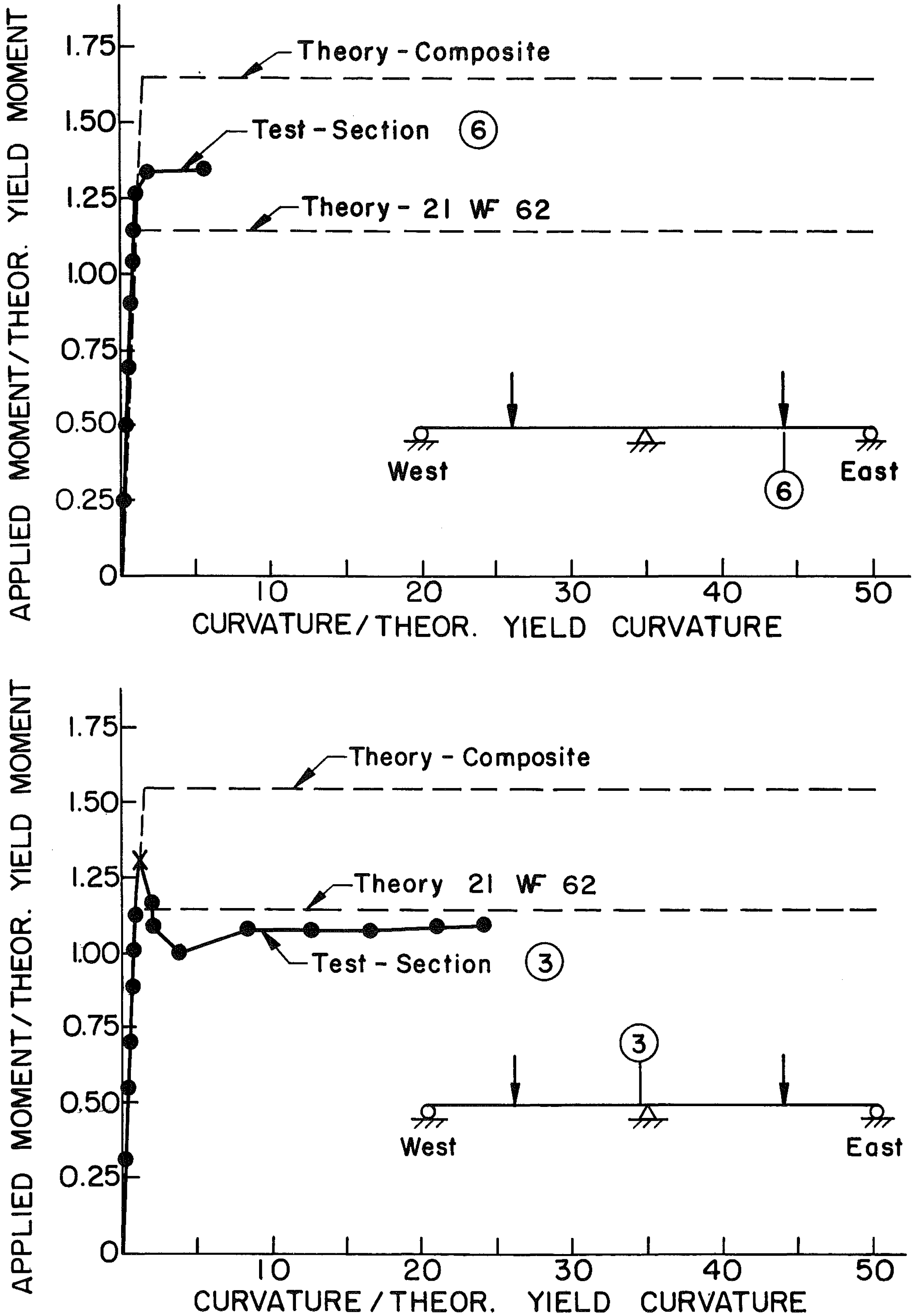

FIG. 9 - CC-1F MOMENT-CURVATURE CURVES

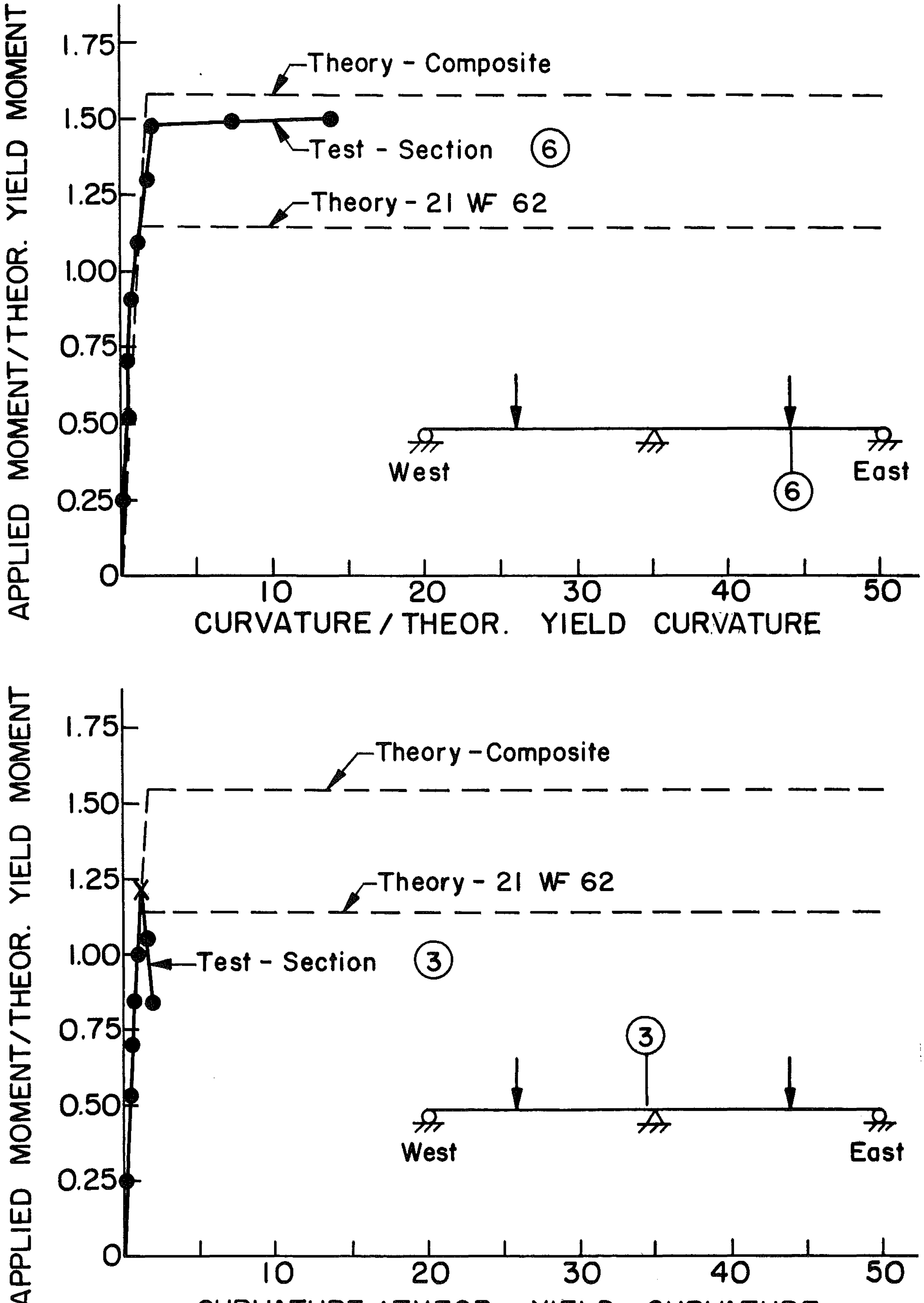

FIG. 10 - CC-2F MOMENT - CURVATURE CURVES

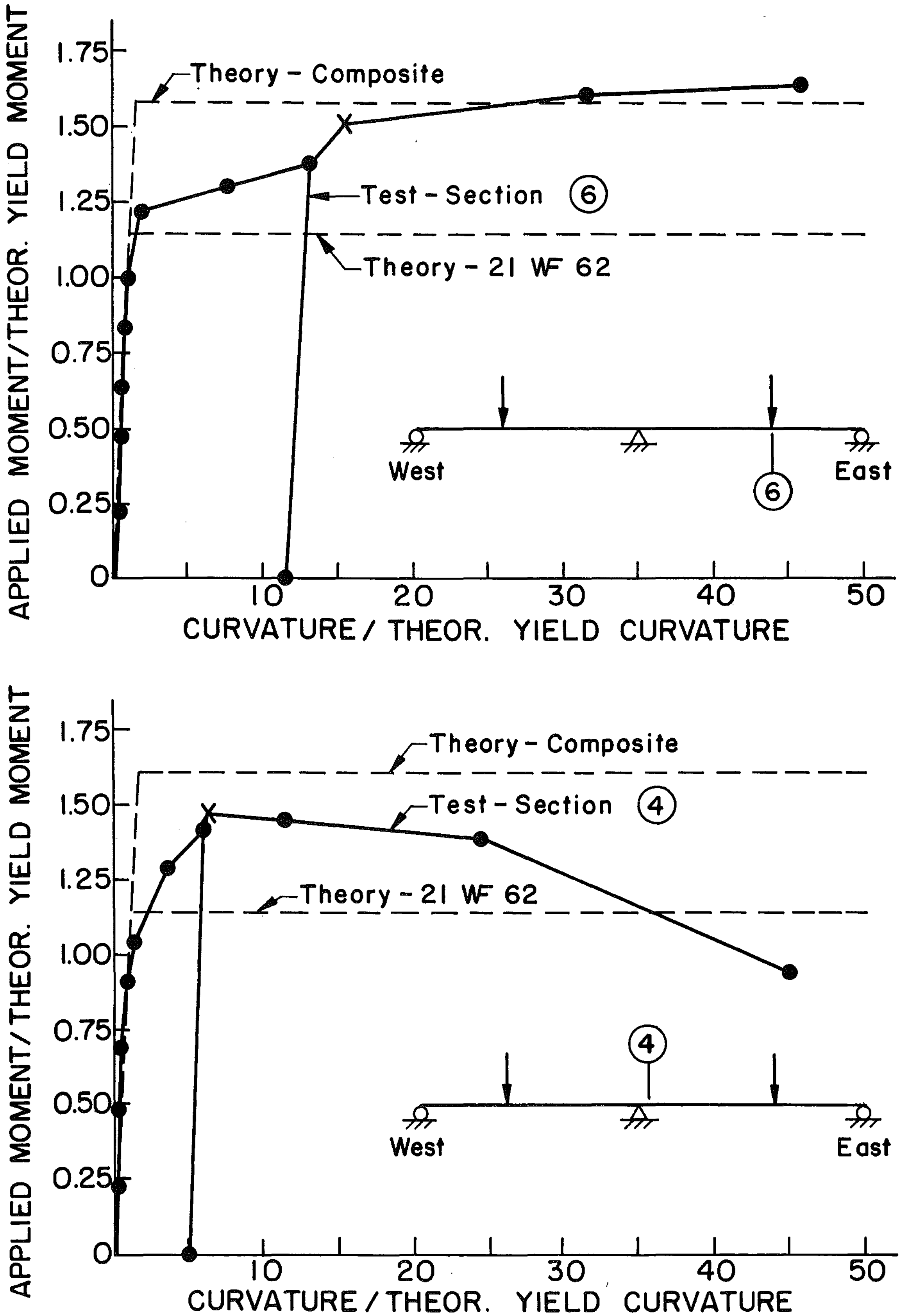

FIG. 11 - CC-3S MOMENT - CURVATURE CURVES

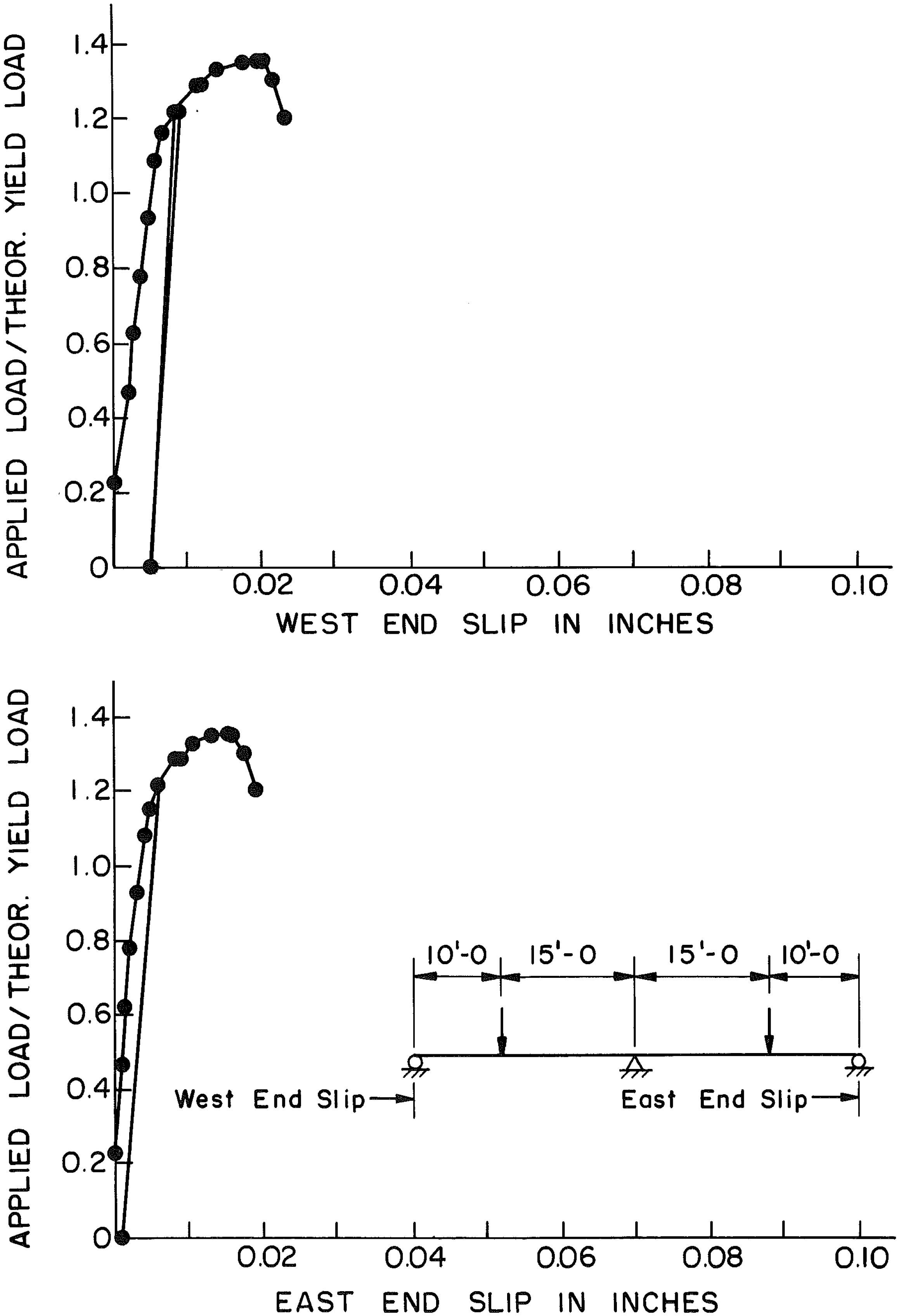

FIG. 12 - CC-2F LOAD SLIP CURVES

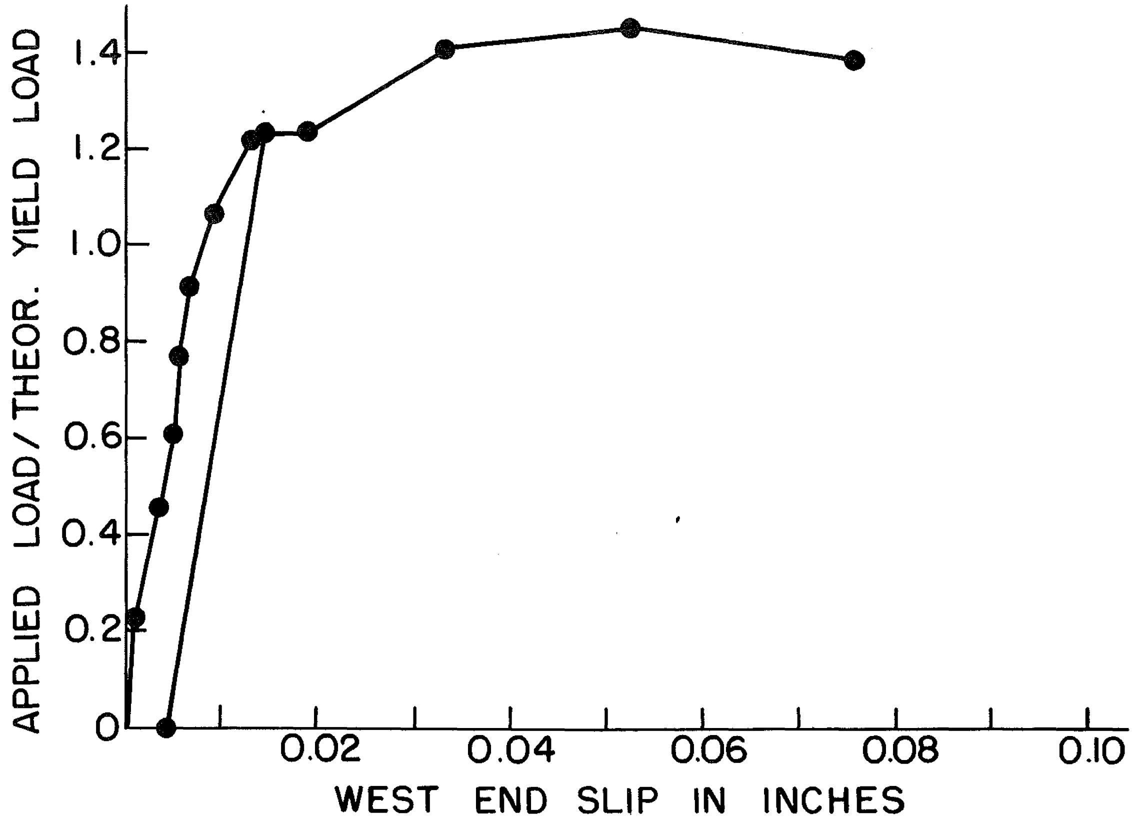

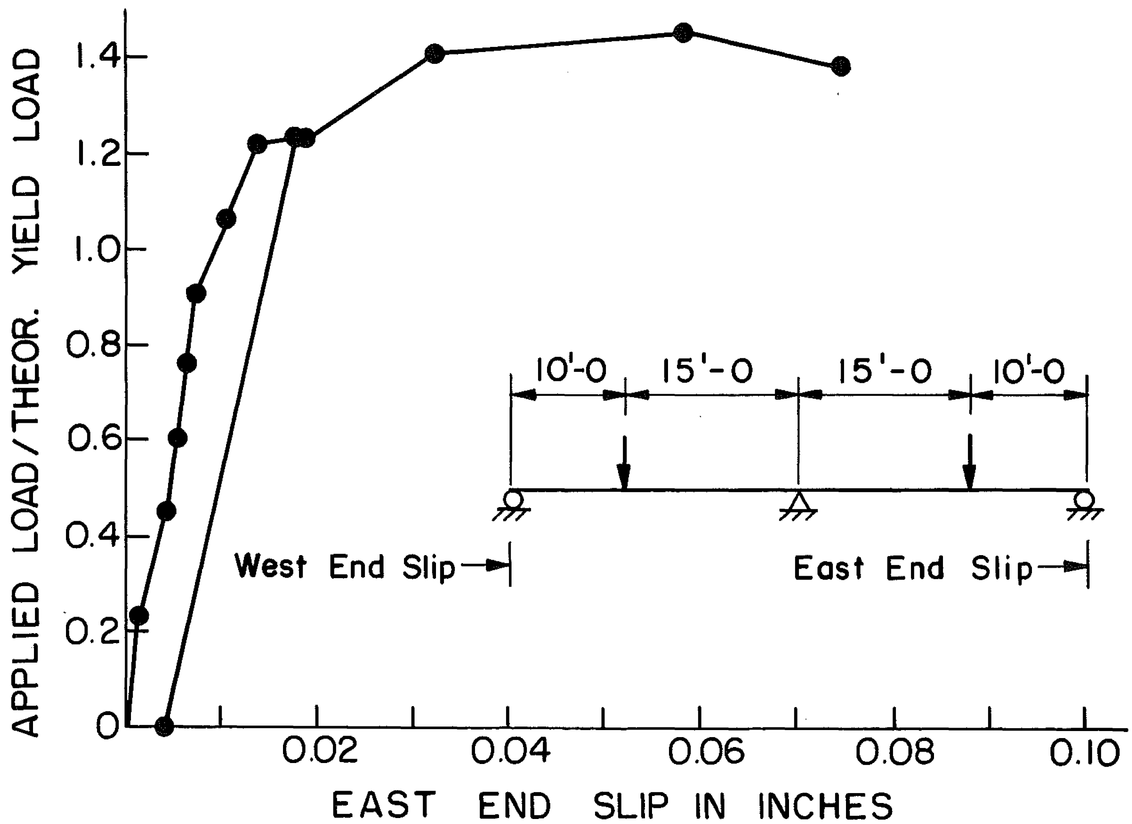

FIG. 13 - CC-3S LOAD SLIP CURVES

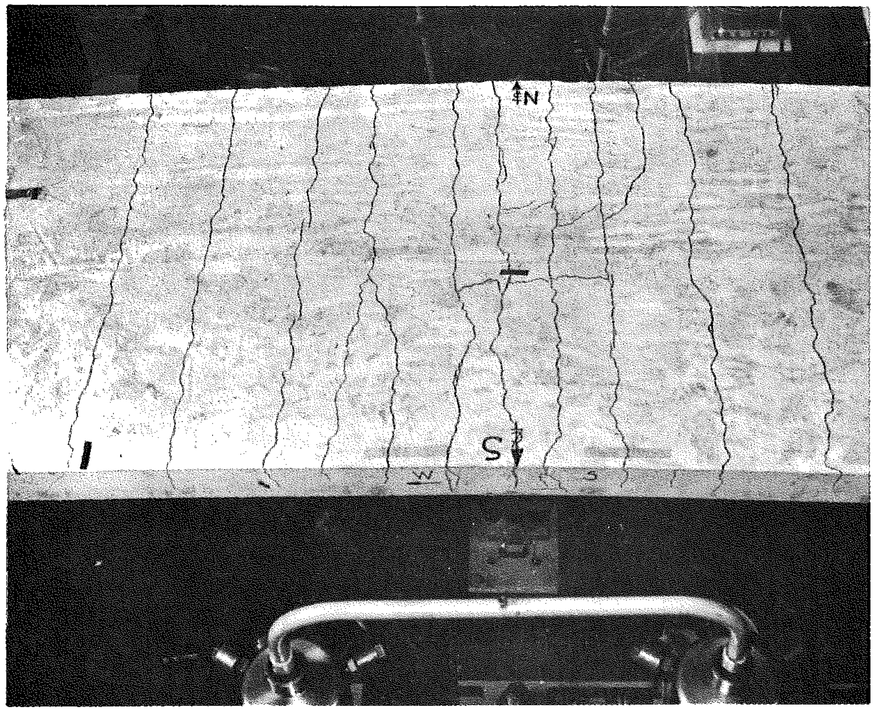

CC-1F

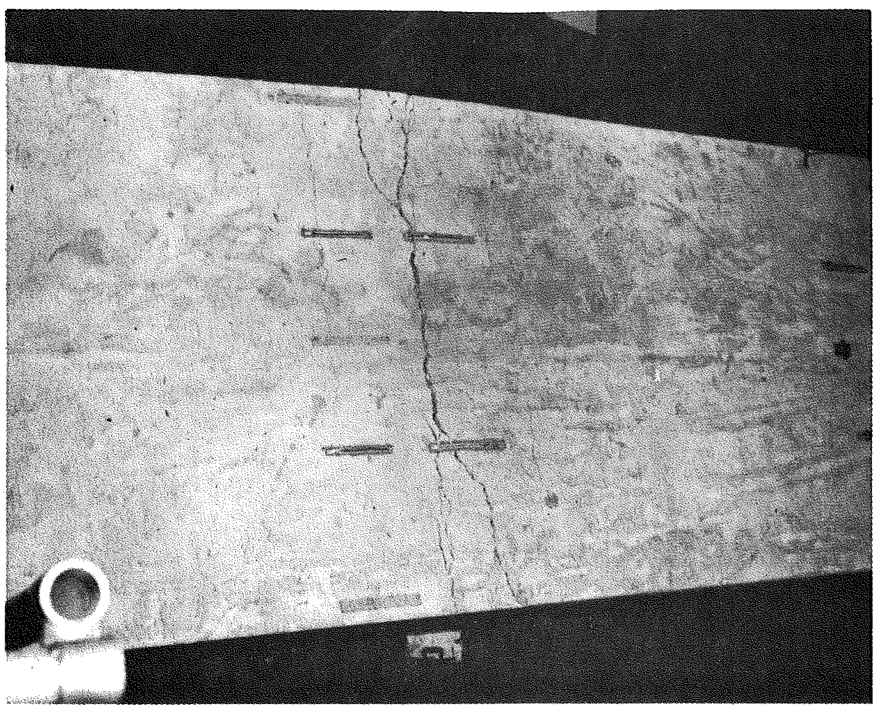

CC-2F

FIG. 14 - CRACK DISTRIBUTION IN NEGATIVE MOMENT REGIONS

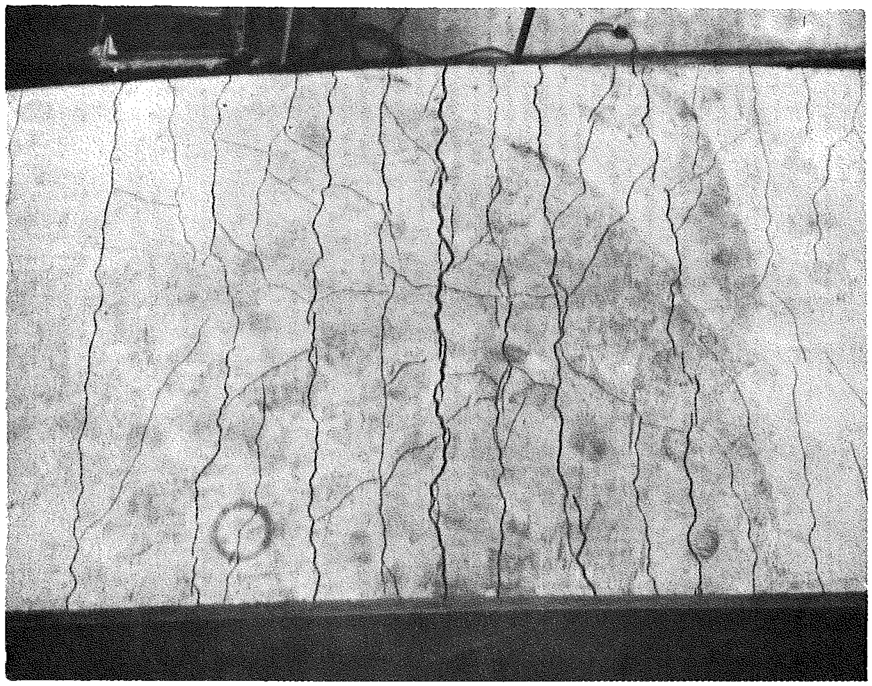

CC-3S

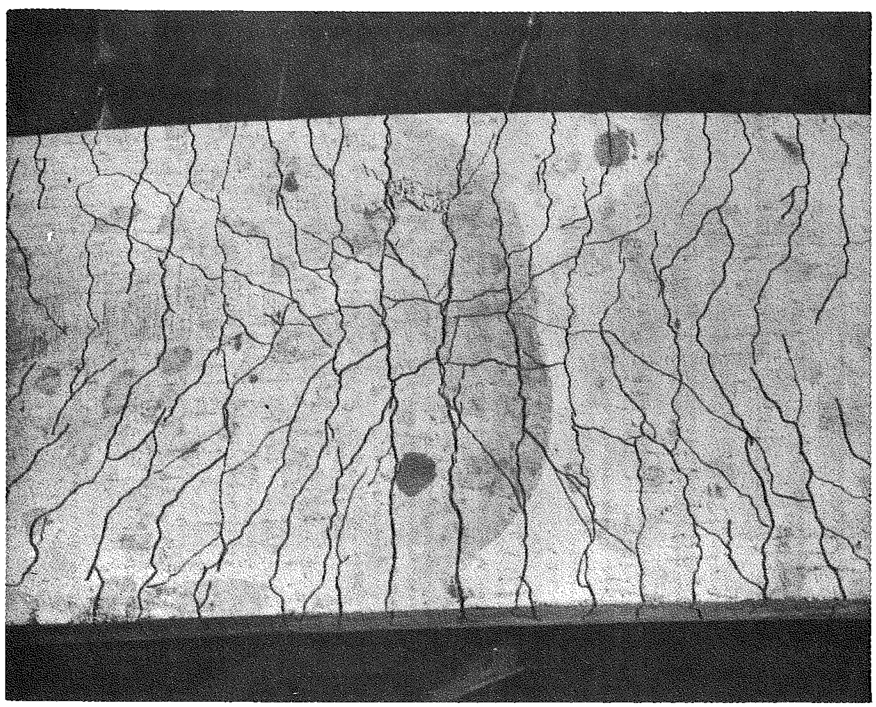

CC-4S

FIG. 15 - CRACK DISTRIBUTION IN NEGATIVE MOMENT REGIONS

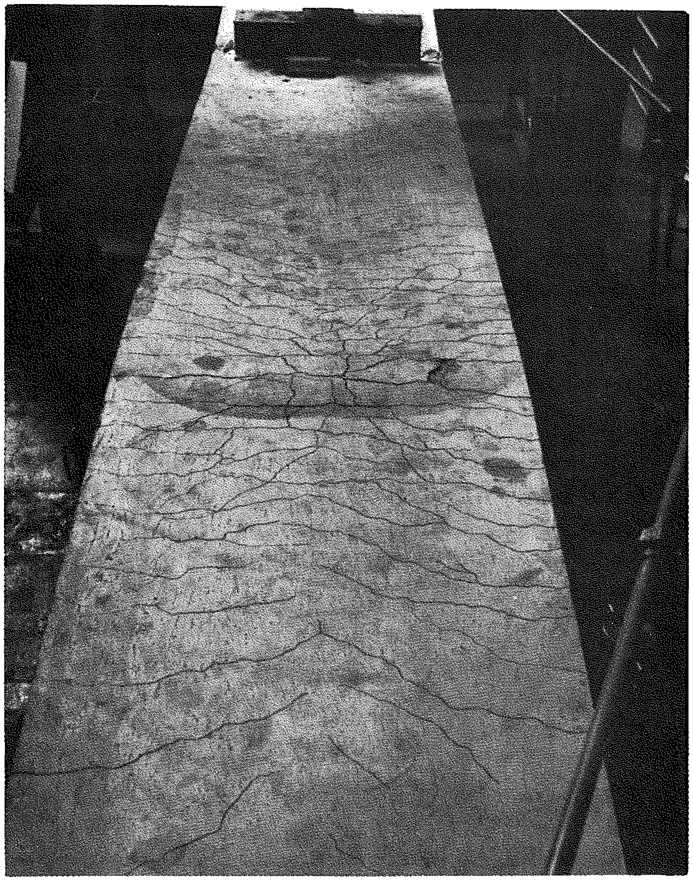

CC-4S

FIG. 16 - CC-4S SPALLING OF SLAB

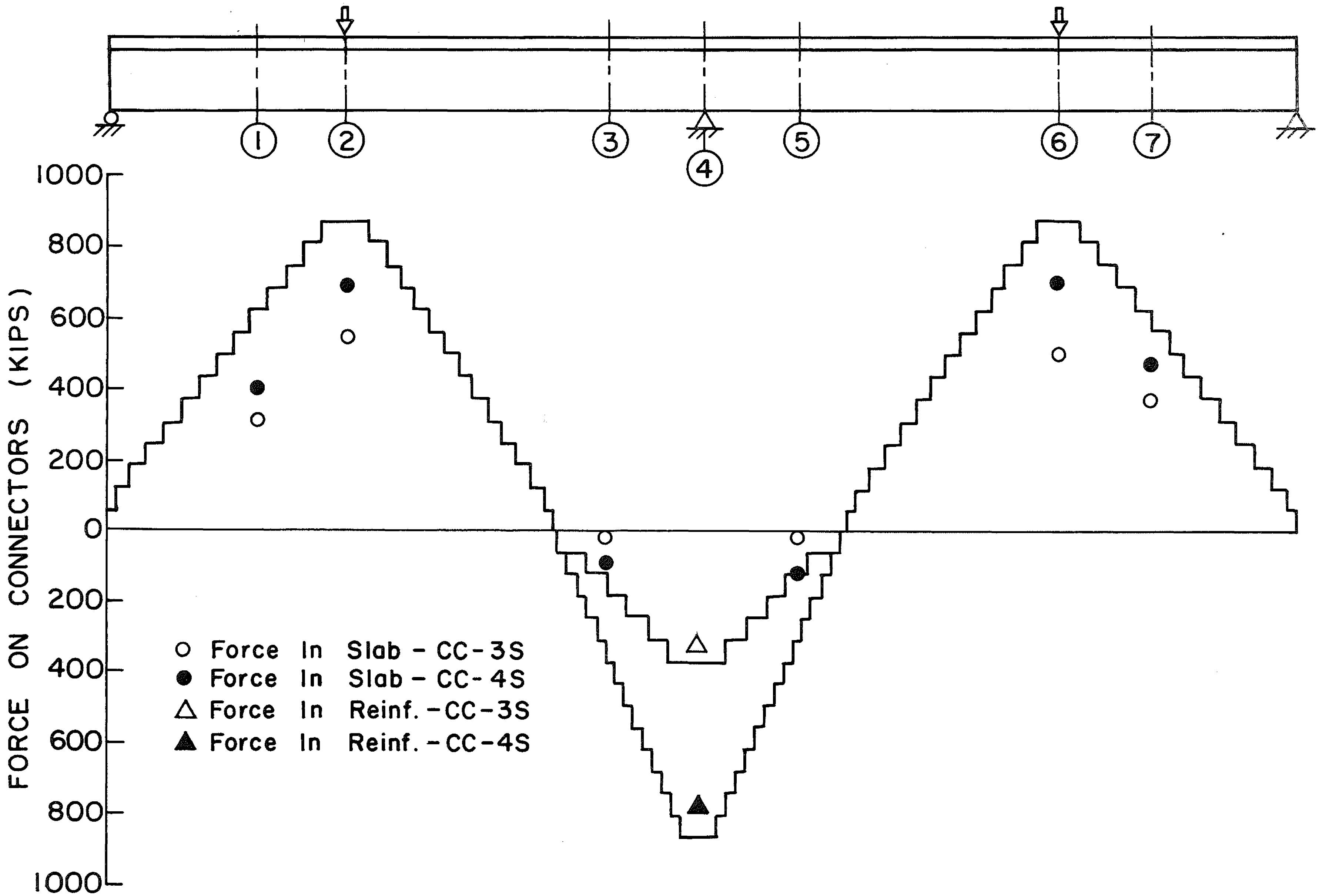

FIG. 17 - CUMULATIVE RESISTANCE OF STUD CONNECTORS - CC-3S AND CC-4S

11. REFERENCES

1. Beedle, L. S., et al,
   STRUCTURAL STEEL DESIGN, (CHAPTER 13) ed. by Lambert Tall, Ronald Press Company, New York. 1964

2. American Association of State Highway Officials
   STANDARD SPECIFICATIONS FOR HIGHWAY BRIDGES, Ninth Edition, Washington, D.C. 1966

3. Viest, I. M., Fountain R. S., and Siess, C. P.
   DEVELOPMENT OF THE NEW AASHO SPECIFICATIONS FOR COMPOSITE STEEL AND CONCRETE BRIDGES, Highway Research Board, Bulletin 174, 1958

4. Slutter, R. G., and Fisher J. W.
   FATIGUE STRENGTH OF SHEAR CONNECTORS, Highway Research Record No. 147, Highway Research Board, 1966, pp. 65 - 88

5. Daniels, J. Hartley, and Fisher J. W.
   FATIGUE BEHAVIOR OF CONTINUOUS COMPOSITE BEAMS, Fritz Engineering Laboratory Report No. 324.1. 1966

6. Siess, C. P., and Viest, I. M.
   STUDIES OF SLAB AND BEAM HIGHWAY BRIDGES: V: TESTS OF CONTINUOUS RIGHT I-BEAM BRIDGES, Bulletin No. 416, University of Illinois Engineering Experiment Station, 1953

7. Slutter, Roger G., and Driscoll, George C. Jr.
   FLEXURAL STRENGTH OF STEEL-CONCRETE COMPOSITE BEAMS, Journal of the Structural Division ASCE, Vol. 91, No. ST2. 1965

8. Culver, Charles; Zarzeczny, Paul J., and Driscoll, George C. Jr.
   TESTS OF COMPOSITE BEAMS FOR BUILDINGS, Fritz Engineering Laboratory Report No. 279.6. 1961

9. Iwamoto, K.
   ON THE CONTINUOUS COMPOSITE GIRDER, Highway Research Board, Bulletin 339. 1962

10. Tachibaba, Y., Kondo, K., and Ito, K.
    EXPERIMENTAL STUDY ON COMPOSITE BEAMS PRESTRESSED WITH WIRE CABLES, International Association for Bridge and Structural Engineering, Preliminary Publication of the Seventh Congress. 1964

11. Barnard, P. R., and Johnson, R. P.
PLASTIC BEHAVIOR OF CONTINUOUS COMPOSITE BEAMS, Proceedings, Institution of Civil Engineers, Vol. 32, October 1965. pp. 161 - 179

12. Johnson, R. P., VanDalen, K., and Kemp, A. R.
ULTIMATE STRENGTH OF CONTINUOUS COMPOSITE BEAMS, Progress Report, British Constructional Steelwork Association Conference, September 1966

13. Galambos, T. V., and Lay, M. G.
STUDIES OF THE DUCTILITY OF STEEL STRUCTURES, Journal of the Structural Division, Proc. ASCE Vol. 91, ST4. August 1965. p. 125

14. Lay, M. G.
FLANGE LOCAL BUCKLING IN WIDE-FLANGE SHAPES, Journal of the Structural Division, Proc. ASCE, Vol. 91, No. ST6, December 1965, p. 95

15. Lay, M. G., and Galambos, T. V.
INELASTIC BEAMS UNDER MOMENT GRADIENT, Journal of the Structural Division, Proc. ASCE, Vol. 93, No. ST1, February 1967, p. 381

16. Beedle, L. S., et al.
STRUCTURAL STEEL DESIGN, (Chapter 17), ed. by Lambert Tall, Ronald Press Company, New York. 1964

17. Driscoll, G. C. Jr., et al.
PLASTIC DESIGN OF MULTI-STORY FRAMES - LECTURE NOTES, (Chapter 3), Fritz Engineering Laboratory Report No. 273.20 Lehigh University, 1965. (Presented at the 1965 Summer Conference on the Plastic Design of Multi-Story Frames, Lehigh University, August 24 - September 2, 1965

18. American Institute of Steel Construction
STEEL DESIGN MANUAL, AISC, 6th Edition, New York, 1964

19. American Institute of Steel Construction
COMMENTARY ON PLASTIC DESIGN IN STEEL, Manuals of Engineering Practice, No. 41, 1961

20. Daniels, J. Hartley, and Fisher, John W.
STATIC BEHAVIOR OF COMPOSITE BEAMS WITH VARIABLE LOAD POSITION, Fritz Engineering Laboratory Report No. 324.3, Lehigh University, March 1967.